THESIS

SNOWMELT AND RAINFALL RUNOFF IN BURNED AND UNBURNED CATCHMENTS AT THE INTERMITTENT-PERSISTENT SNOW TRANSITION, COLORADO FRONT RANGE

Submitted by

Adam Johnson

Department of Ecosystem Science and Sustainability

In partial fulfillment of the requirements

For the Degree of Master of Science

Colorado State University

Fort Collins, Colorado

Spring 2016

Master's Committee:

Advisor: Stephanie Kampf

Steven Fassnacht
Jeffrey Niemann

ABSTRACT

SNOWMELT AND RAINFALL RUNOFF IN BURNED AND UNBURNED CATCHMENTS AT THE INTERMITTENT-PERSISTENT SNOW TRANSITION, COLORADO FRONT RANGE

Winter snowmelt and summer monsoonal rains are the dominant sources for streamflow in the Colorado Front Range, and wildfire can greatly affect the hydrologic regime through which these inputs are delivered to the stream. However, the specific changes to the hydrologic processes that drive runoff production made by wildfire are not clearly understood. This research examines how wildfire affects the timing and magnitude of runoff production from snowmelt and rainfall by comparing four catchments in and near the High Park Fire area, two burned and two unburned, at the intermittent-persistent snow transition.

Catchments were instrumented to monitor snow accumulation and ablation, rainfall, soil moisture, soil and air temperature, and streamflow response throughout water year 2015. These data were then utilized to determine the primary mechanisms of seasonal runoff generation and the magnitude of that runoff from each catchment. Runoff remained very low at all catchments during winter months. Spring snowmelt runoff in the form of lateral subsurface flow dominated catchment hydrographs for the water year. Following spring snowmelt, runoff production transitioned to a rainfall-dominated, drier summer period. During this time, limited infiltration excess overland flow was produced from high intensity rainfall events.

Results of this research suggest that the loss of canopy cover due to wildfire may result in increased snowpack density and more intermittent snowpack throughout the winter months. Burned monitoring sites also maintained higher soil moisture than unburned sites, but this may be a function of site-specific variability rather than burning. Elevated soil moisture at burned sites did not translate to consistently higher runoff production. Both total runoff production and runoff ratios were highest in the high elevation unburned site with the highest snow persistence and the lowest elevation burned site with low snow persistence. During the one high intensity rain event that affected all catchments, burned catchments experienced an increase in discharge above baseflow of a greater magnitude than unburned sites. Overall, all catchments monitored showed site specific characteristics that defied easy classification but illustrated local variability in the hydrologic variables monitored.

ACKNOWLEDGMENTS

I'm grateful to the National Science Foundation for funding this research, through grants DIB-1230205 and DIB-1339928. Additional support for the research came from the Warner College of Natural Resources mini-grant program. I'd like to thank the U.S. Forest Service for supporting access to research sites and for allowing me to instrument and monitor catchments on federal lands. I'd also like to thank Amy and Todd Williams, Ray Ramos, and the wardens of Sky Corral Ranch for allowing me to cross private property in order to access the research catchments.

Additionally I'd like to thank everyone who lent insight on my research, including Lee MacDonald, Tim Covino, John Stednick, Sandra Ryan, and Chuck Rhoades. Special thanks to Codie Wilson, John Hammond, Sarah Schmeer, Ryan Webb, and Josh Faulconer for help both in the field and at the computer. I want to thank everyone who helped with field work, including Steven Filippelli, Miranda Middleton, Freddy Saavedra, Clay Bliss, Lindsey Middleton, Cassidi Rosenkrance, Emily Chavez, Erik Sandquist, Archer and many others too numerous to name here.

Finally, a special thanks to my committee members Steven Fassnacht, who kept me sane and made snow exciting, and Jeffrey Niemann. Boundless thanks to my adviser, Stephanie Kampf, without whose support and faith I couldn't have even begun this project, much less completed it. Last in mention but foremost in my heart, thanks to my wife, Katie, and my daughter, BonnyMae. I love you both, and I would not be where I am now without you.

TABLE OF CONTENTS

LIST OF TABLES

LIST OF FIGURES

1 INTRODUCTION

Winter snowmelt and summer storms are the dominant sources of streamflow in the mountains of the Colorado Front Range (Colorado Climate Center, 2015). Wildfire changes the hydrologic regime of this region by removing forest canopy and ground cover, decreasing interception of snow and rainfall, and increasing overland flow response to snowmelt and summer rains (Westerling et al., 2006). Greater overland flow causes increased hillslope erosion and flashier streamflow response, which has ramifications for sediment transport, channel geomorphology, and downstream water quality. While the erosion and sedimentation consequences of wildfire have been widely studied in this region (e.g. Benavides-Solario and MacDonald, 2005; Moody et al., 2005; Robichaud, 2005; Wagenbrenner et al., 2006), less research has been done on the hydrologic processes that drive these responses. This study examines how wildfire affects hydrologic response by comparing burned and unburned catchments in and near the 2012 High Park Fire in northern Colorado. The primary purpose of the study is to determine how wildfire affected the timing and magnitude of runoff from snowmelt and rainfall. To accomplish this, the research evaluates differences between snow accumulation and ablation, rainfall, soil moisture, soil and air temperature, and streamflow response across two burned and two unburned research catchments.

2 BACKGROUND

Wildfire can impact many of the hydrologic processes that lead to runoff generation (Table 1). Removal of canopy cover and changes in vegetation and soil properties may result in increases or decreases in the relative magnitude of a number of hydrologic variables. This section describes the nature of these processes in the study area and how they may be affected by wildfire.

Table 1: Conceptual table showing expected changes in a number of hydrologic and hydrologically relevant variables following wildfire. Plus signs (+) indicate and increase and minus signs (-) indicate a decrease.

Variable	Effect of burn
Solar insolation	**+**
Interception	**-**
Snow accumulation	**+**
Snow ablation rate	**+**
Snow persistence	**-**
Peak SWE	**+/-**
Evaporation	**+**
Transpiration	**-**
Infiltration	**-**
Runoff	**+/-**

2.1 Snow accumulation and melt

Inputs to streamflow in the Colorado Front Range can be either snowmelt, rainfall, or a combination of both. Snowfall begins as early as October for some areas of the Colorado Front Range, but greatest spatial extent of snow cover is seen December through February (Richer et al., 2013; Moore et al., 2015). Snow cover is strongly correlated to elevation and air temperature,

two collinear factors that result in greater amounts of precipitation falling as snow, greater accumulation, and increased snowpack persistence at high elevations (Richer et al., 2013). Previous studies divided the region into snow zones based on mean annual snow persistence during 1 January – 3 July. These studies used NASA's Moderate Resolution Imaging Spectroradiometer (MODIS) snow covered area data from 2000 – 2010 to identify three primary snow zones (Richer et al., 2013; Moore et al., 2015). The persistent snow zone (PSZ) is the highest elevation zone where snow cover is present every winter, lasts into late spring, and where the timing of ablation does not change with elevation. The transitional snow zone (TSZ) is a middle elevation zone where snow cover is present every winter, lasts through winter, and ablation occurs later with increasing elevation. The intermittent snow zone (ISZ) is the lowest elevation zone where snow cover is more inconsistent and does not always last continuously through winter. Despite the common use of 1 April for peak SWE, peak SWE for this region varies with elevation between mid-April and mid-May, driven by spring snowfall. Complete ablation of the snowpack typically occurs in May or June, with the region remaining snow-free from July through September (Richer et al., 2013).

At fine scales within a given snow zone, canopy cover, interception, and sublimation control snowpack accumulation. Forest canopy can intercept and sublimate 25-45% of snowfall (Hedstrom and Pomeroy, 1998), so when wildfire removes canopy, canopy interception decreases, and greater solar insolation affects snow accumulation and ablation. Removal of forest cover can reduce spatial variability in the snowpack because canopy cover and vegetation vary the magnitude and distribution of the snowpack (Harpold et al., 2014). Prior studies have

shown that snow accumulation in wildfire areas has later accumulation onset, greater overall accumulation, and more fluctuation in soil temperature through the accumulation season (Molotch et al., 2009). However, the effect of wildfire on peak snow depth varies regionally. Burles & Boone (2011) found higher peak snow depth following wildfire at high latitudes and elevations in Alberta, Canada, while Harpold et al. (2014) found lower peak snow depth following wildfire in the warmer Jemez Mountains of New Mexico. Because of the greater influence of solar radiation in burned areas, climates with high solar radiation can experience more rapid ablation that varies by slope and aspect. Ebel et al. (2012) found that aspect was the primary control on snowpack ablation immediately following a wildfire in the Colorado Front Range, with south-facing slopes experiencing full ablation many times throughout the season while north-facing slopes developed some continuous or nearly continuous snowpack. Over time this aspect dependence may lessen due to the return of vegetation, but research still suggests that even after 2-5 years of recovery, full ablation of the snowpack in a burned area may occur weeks earlier than in an unburned area, because of less canopy and higher energy availability (Burles & Boone, 2011; Winkler, 2011). Because of the combined effects of wildfire on snow accumulation and ablation, snow water equivalent (SWE) shows a varying relation to wildfire, with some studies (Burles & Boone, 2011; Winkler, 2011) finding increases in SWE as high as 58% over unburned areas and other studies (Drake et al., 2008) finding decreases in SWE following a fire.

During the ablation season, snowmelt water begins to move towards the stream via lateral subsurface flow and/or overland flow (Dunne, 1978; Kampf et al., 2015). Some studies

have found that infiltration excess overland flow (IEOF) is rare during snowmelt except where soils are frozen (Wilcox et al., 1997; Bayard et al., 2004; Smith et al., 2014). Saturation excess overland flow (SEOF) is possible, particularly where melt of a deep snowpack leads to sustained input and soil saturation (Dunne & Black, 1971; Kampf et al., 2015). Where snowpacks are not as deep, lateral subsurface flow (LSSF) is likely the dominant mechanism of streamflow generation from snowmelt. For a semi-arid mountain region in Idaho, McNamara et al. (2005) defined a transition from a winter wet, low-flux period into a spring wet, high flux period driven by snowmelt. During the wet period, soil moisture movement changed from primarily vertical to primarily lateral, resulting in snowmelt-driven lateral subsurface flow to the stream. Delivery of snowmelt water to the stream depends on the maintenance of spatial connectedness in regions of soil moisture. Prior studies in the Dry Creek Experimental Watershed, near Boise, Idaho, found that the strongest control on this connectivity is spatial distribution of snow, followed by slope position, soil texture, and soil depth (Seyfried et al., 2009; Williams et al., 2009).

In unburned areas, vegetation affects soil moisture patterns by changing the spatial distribution of snow, creating preferential pathways into subsurface storage and modifying evapotranspiration (ET) (Hunsaker et al., 2012). Differences in snow accumulation and melt water delivery patterns can result in changes in hydrologic connectivity through hillslopes (Hinckley et al., 2014). The decreases in snowpack spatial variability and increases in available energy seen in burned areas can lead to considerable differences in soil moisture and stream discharge. Burned areas may have a different sequence of inputs into soil moisture than

unburned areas due to a cycle of rapid accumulation and ablation (Ebel et al., 2012), which can affect both hydraulic connectivity and lateral flow in the subsurface. More rapid evaporation and draining from soils in burned areas can further decrease hydraulic conductivity across hillslopes (Ebel et al., 2012).

2.2 Rainfall

In the Colorado Front Range, rainfall in summer months often takes the form of high-intensity convective storms (Osborne et al., 1972; Wilcox et al., 1997; Ebel et al., 2012). The transition from snow to rain may begin as early as April at lower elevations, though complete lack of new snowfall across all elevations in the region may not occur until mid to late June in many years (Richer et al., 2013). Rainfall in this region is also highly spatially variable, with small-scale precipitation variability influenced by topographic variation (Osborne and Lane, 1972; Linderson, 2003; Smith et al., 2014). This spatial variability may change with event type and magnitude (Smith et al., 2014). Vegetation also plays a key role in both the spatial variability of rainfall reaching the surface and in the spatial distribution of soil moisture. Tree canopy in semiarid regions can intercept as much as 60% of rainfall (Martinez-Meza and Whitford, 1996). Tree roots also provide preferential flow paths into subsurface storage and utilize soil moisture in transpiration. Trees and other vegetation also produce an organic rich layer on the forest floor, which stores rainwater and impedes overland flow (Martin and Moody, 2001).

Runoff production from rainfall events is closely related to event magnitude and antecedent soil moisture conditions (Dunne and Black, 1970). Runoff generation can be in the

form of SEOF, IEOF, or LSSF. Wilcox et al. (1997) found that semiarid hillslopes experienced IEOF following high intensity storms, and no SEOF was observed. They concluded that the primary mechanism for movement of water once saturation is reached during rain events in semiarid regions is LSSF. Though no SEOF was observed by Wilcox et al. (1997), long duration frontal storms or rainfall occurring on saturated soils (e.g. following snow melt) may produce SEOF on shallow, low-permeability soils (Lopes and Ffolliott, 1993).

Wildfire can completely alter forest canopy, forest floor, and near-surface soil conditions (Shakesby and Doerr, 2006). This decreases interception, increases magnitude, and quickens the timing of rainfall introduction to the soil surface. Wildfire burns or vaporizes the organic layer covering the soil surface (Pierson et al., 2001; Ebel et al., 2012). Burning of this organic layer replaces it with an ash layer, affecting initial water storage capacity prior to rainfall and, in turn, the threshold for runoff generation (Ebel et al., 2012). Vaporization of the organic layer releases organic compounds which can result in hydrophobicity at the soil surface, blocking water infiltration into the soil (Robichaud, 2000). Soil infiltration and subsurface moisture storage may also be affected by wildfire. Martin and Moody (2001) found a reduction in steady state infiltration at burned locations following a wildfire compared to unburned locations, citing increased water repellency, sealing of soil pores by hydrophobic compounds, and reduced soil porosity due to combustion of organic materials in the soil. Garcia-Corona et al. (2004) also found a reduction in hydraulic conductivity in near surface soils (0-5cm) that resulted in decreased infiltration which facilitates surface runoff. These wildfire-related changes in vegetation and soil properties are transient, showing greatest effect immediately following a fire

and lessening over time. Pre-fire conditions of infiltration are usually restored within three to five years following the fire (Moody and Martin, 2001; Pierson et al., 2001). Moody and Martin (2001) found that storms with a 30-minute rainfall intensity (I_{30}) of about 1cm/h produced more runoff and higher peak discharge one year after a fire than storms with the same intensity produced in the third and fourth years following a fire, potentially due to changes in infiltration.

In the body of literature cited above, no previous study has attempted to synthesize the hydrologic outcomes of all three factors: snowmelt, rainfall, and wildfire. This research examines changes in the timing and magnitude of runoff from burned and unburned catchments during snowmelt and during rain storms in an area near the boundary between seasonally intermittent and seasonally persistent snow cover.

3 SITE DESCRIPTION

The High Park Fire burned in June of 2012 in the foothills and mountains west of Fort Collins, CO, sparked by a lightning strike following an unseasonably dry spring (Colorado Climate Center, 2015). The fire burned for 21 days from spark to full containment and affected over 353km^2, making it the second largest fire by area in Colorado state history (High Park Fire BAER Report, 2012). Of this 353km^2, 21% of the area was unburned, 24% had low severity burn, 15% moderate severity burn, and 40% high severity burn (Stone, 2015). Vegetation prior to the fire consisted of mixed forests of lodge pole pine, ponderosa pine, and Douglas-fir. Stands of aspen were interspersed in forests across the elevation gradient. These vegetation types persist in areas that were unburned and areas outside of the fire-affected zone.

For this study, four study catchments were selected in the Cache la Poudre watershed, two burned catchments within the High Park Fire and two unburned catchments near Pingree Park Road west of the fire-affected area (Figure 1). Catchments were selected near the intermittent-persistent snow transition delineated in Moore et al. (2015). Moore et al. (2015) found that mean annual 1 January – 3 July snow persistence of 0.50 roughly separates areas with persistent winter snow from those with intermittent winter snow. Catchments were chosen to have mean annual snow persistence near this threshold, placing them in or near the transitional snow zone (TSZ) between persistent and intermittent snow zones. Unburned transitional (UT) and unburned intermittent (UI) are the unburned catchments, with UT located in the TSZ and UI straddling the TSZ and the intermittent snow zone (ISZ). Burned transitional

(BT) and burned intermittent (BI) are the burned catchments, with BT located in the TSZ and BI in the ISZ.

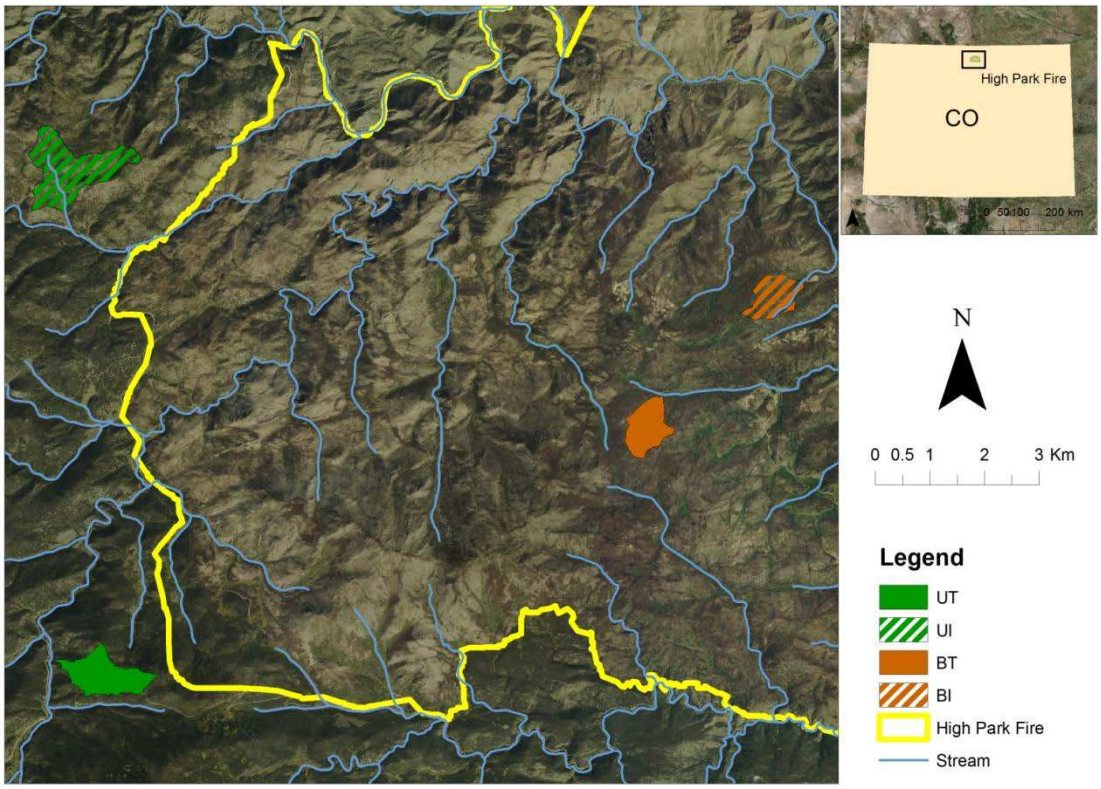

Figure 1: Map of the western High Park Fire burn area showing research catchments and location of the study area in Colorado; satellite imagery from ArcMap (2014).

Catchment areas range from 0.60km^2 to 1.53km^2 (Table 2). Elevations for the four catchments range from 2230m to 2868m. Mean elevation for the higher elevations sites is similar, 2671m for UT and 2601m for BT. Mean elevation for the lower elevation sites shows more discrepancy, 2507m for UI and 2382m for BI, but both lower elevations sites represent the ISZ. Mean annual P, derived from Parameter- Elevation Regressions on Independent Slopes Model (PRISM) normals for 1981-2010, is 513-561mm at high elevation sites and 462-503mm at

low elevation sites (PRISM Climate Group, 2015). Mean annual 1 January – 3 July snow persistence from 2000 - 2010 was 10% higher at higher elevation sites for both unburned and burned catchments.

Table 2: Summary characteristics of burned (B) and unburned (U) catchments.

Site	Area[1] (km^2)	Elevation[1] (m)		Average Slope[1] (deg.)	Mean Annual P[2] (cm)	Mean Annual Snow Persistence[3]
		Mean	Range			
UT	0.84	2671	2513-2868	15.3	51.3	0.60
UI	1.53	2507	2387-2631	14.1	46.2	0.50
BT	0.88	2601	2420-2791	20.6	56.1	0.53
BI	0.60	2382	2230-2505	17.5	50.3	0.43

[1] area, elevation, and slope determined in ESRI ArcGIS using NEON 1m LiDAR DTM for UI, BT, BI and using NED 1arcsec DEM for UT
[2] mean annual precipitation (P) determined using PRISM normals for 1981-2010
[3] mean annual 1 January – 3 July snow persistence derived from Moore et al., 2015

Dominant soil textures at burned study catchments are more diverse than at unburned study catchments (USDA/NRCS, 2015). Soils at BT and both unburned sites are dominated by well-drained gravelly sandy loam with depths of 50 – 150cm to a restrictive layer. UI also has a poorly drained silt loam with a depth > 200cm underlying the majority of the stream channel. BI is dominated by well-drained sandy clay loam with depths ranging 50 – 200+cm.

Average slope for each site is given in Table 2, and all range from 14-21°. Burned sites have higher slopes than unburned sites, and higher elevation sites 5-8% greater average slopes than their lower elevation counterparts. Dominant aspect for each catchment is shown in Figure 2. All sites are dominated by a south-facing aspect with the exception of BT, which is

dominated by a northeasterly aspect. UT and BT have opposing dominant aspects, with UT primarily southwest-facing and BT primarily northeast-facing. Lower elevation sites are more similar in dominant aspect. UI is primarily south-facing, and BI is primarily east and southeast-facing.

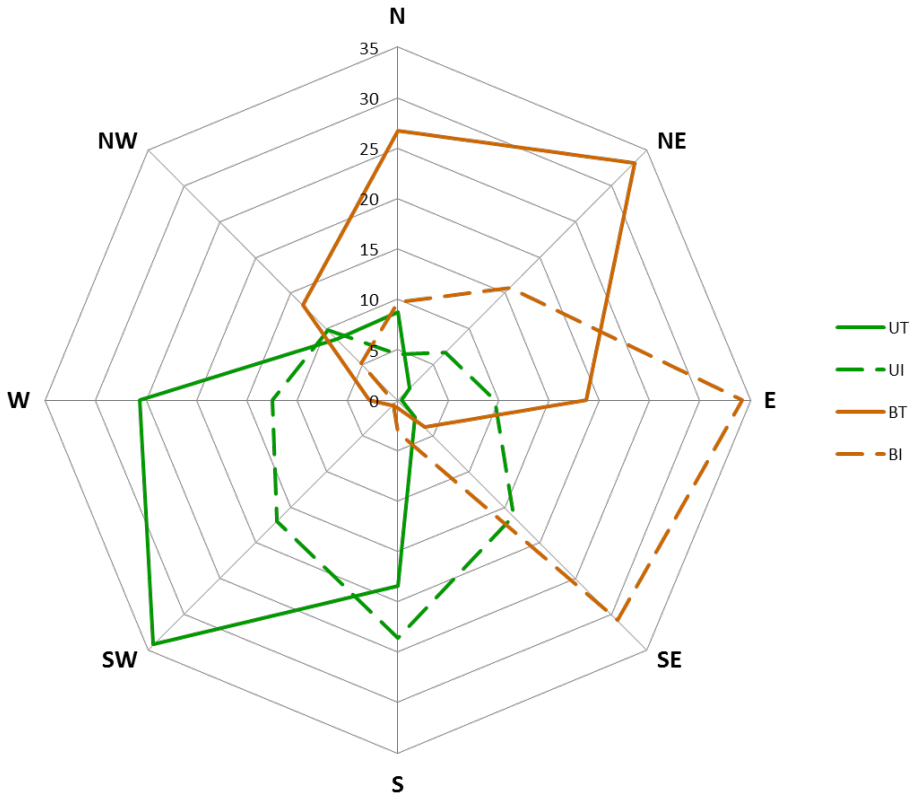

Figure 2: Rose diagram illustrating aspect at UT, UI, BT, and BI; aspect is shown as percentage of watershed area.

For the burned catchments, burn severity, derived from remote sensing data, is shown in Table 3. BT has a greater proportion of unburned area and a lower proportion of high severity burn than BI. However, areas of low and moderate burn severity were a greater percentage of

area at BT than at BI. Overall, 99.4% of BI experienced some degree of burn and 90.2% of the area of BT was burned. Neither UT nor UI were burned during the High Park Fire.

Table 3: Burn severity at BT and BI

Site	Burn Severity[1] (%)			
	No Burn	Low	Moderate	High
BT	10	13	15	62
BI	1	5	12	82

[1] **percentages determined using GIS products from Stone, 2015**

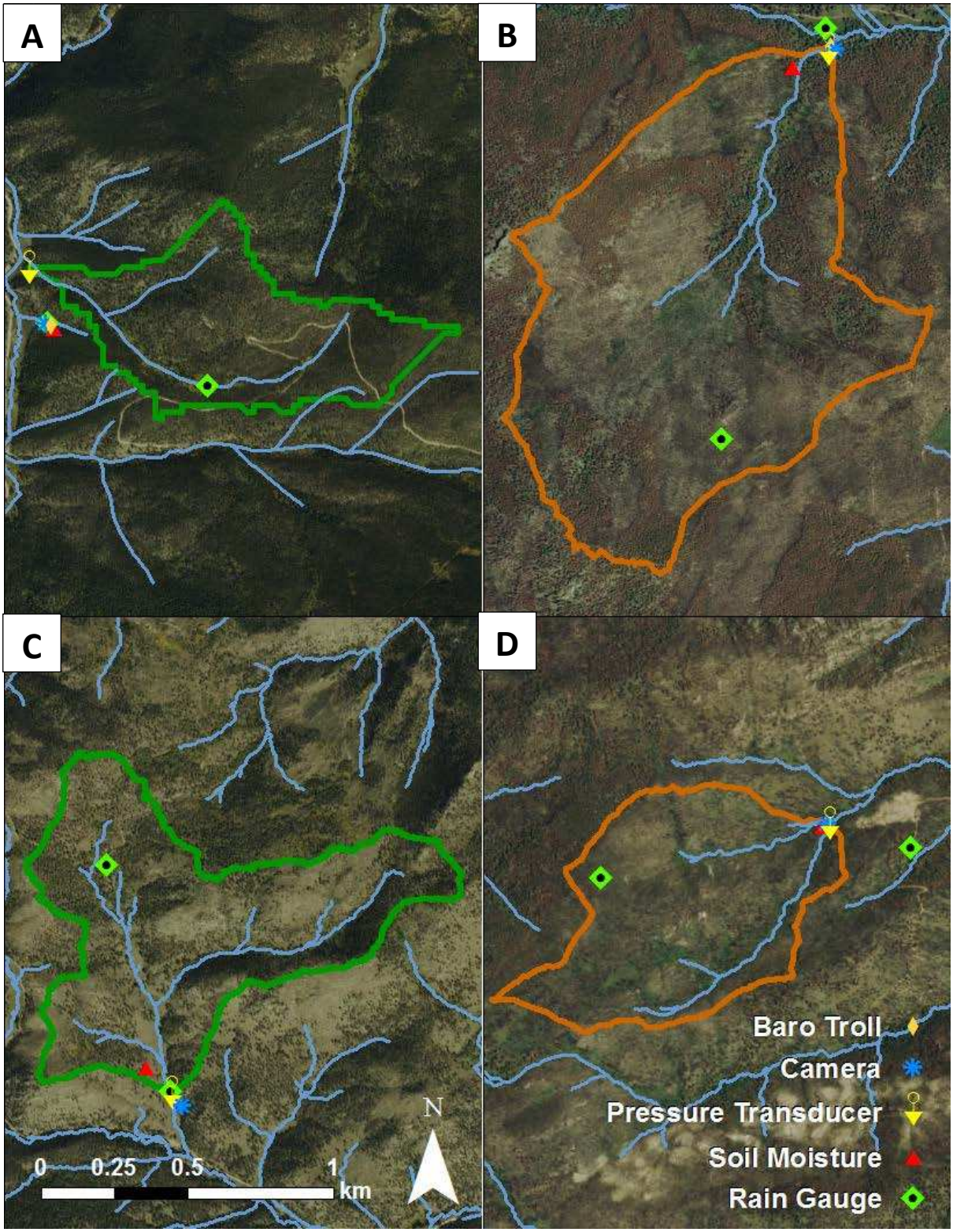

Figure 3: Research catchments and monitoring equipment locations at (A) UT, unburned transitional, (B) BT, burned transitional, (C) UI, unburned intermittent, (D) BI, burned intermittent). Satellite imagery from ESRI ArcMap (2014).

4 METHODS

Field measurements were designed to capture input variables (rain, snow, temperature) and response variables (soil moisture, stream stage) at each study catchment. Field collection and analysis methods are described below.

4.1 Precipitation

Winter precipitation was collected at each site using a NovaLynx Standard Rain and Snow Gauge (NovaLynx Corporation, Grass Valley, CA, USA), which is a collecting rain gauge that requires manual collection of precipitation depths (Figure 4). The funnel and inner cylinder were removed, per manufacturer instruction, to accommodate the collection of winter precipitation. These gauges were mounted at ground level and surrounded with erosion fencing of approximately 1m height to reduce wind effects on snow collection (Fassnacht, 2004). Snow collected into the gauges was retrieved from the gauge and stored in a covered bucket until fully melted. This melt water was then measured using the inner cylinder and a calibrated measuring stick provided by NovaLynx to the nearest 0.1mm. Data were collected every 3 – 6 weeks, depending on site accessibility and time constraints.

Rainfall was collected at each site using both the NovaLynx Standard Rain and Snow Gauge and tipping bucket rain gauges attached to data loggers. The NovaLynx gauge was set up for rainfall collection by reinserting the inner cylinder and funnel within one week of 1 May. The fencing was left in place, and data were collected from the gauge as described above. In addition to this totalizing gauge, two tipping buckets were installed at each site. A RainWise

Rainew 111 tipping bucket rain gauge attached to a RainWise Rainlog data logger was co-located with the totalizing gauge (RainWise Incorporated, Trenton, ME, USA). This tipping bucket (hereafter, TB1) was located near the outlet of each watershed. Data from both TB1 and the totalizing gauge were collected every 3-5 weeks from May through October. A second tipping bucket gauge (TB2) was located centrally in the upper portion of all catchments (Figure 3). This second tipping bucket was added to quantify some of the spatial variability of rainfall across these sites (Osborn et al., 1972). TB2 at all sites was a Texas Electronics TR525I tipping bucket rain gauge (Texas Electronics Incorporated, Dallas, TX, USA) connected to an Onset HOBO Pendant event data logger (Onset Computer Corporation, Bourne, MA, USA). Data from TB2 were collected every 4-6 weeks from snowmelt through October. Both TB1 and TB2 collected at a resolution of 0.254mm per tip.

Figure 4: Initial site install of tipping bucket 1 and the totalizing gauge at BT, fall 2013; site was reconfigured and fencing was added approximately one year later.

The tipping bucket was not useful for snow, and the totalizing rain gauge did not give a continuous time series of data. Therefore, the relative amounts of rain and snow were estimated using PRISM precipitation data combined with a threshold temperature at study sites for separating rain and snow. To identify this threshold temperature, precipitation recorded at TB1, camera observations of snow accumulation and ablation, and estimated precipitation from daily PRISM precipitation data were matched by date for each site. For all dates where TB1 data or camera observations were in agreement with PRISM predictions and a definite determination of precipitation type could be made, a precipitation event was recorded as either snow or rain. Snow days were those with snow accumulation in camera data and precipitation present in PRISM data. Rain days were those with no snow accumulation in camera data and precipitation reported for TB1. Once events were classified as rain or snow, temperature data recorded at each site for dates of precipitation were used in a partition analysis to identify the temperature threshold that best separated rain and snow at the research catchments. This partition analysis identified a threshold temperature for the transition from snow to rainfall of 2.1˚C. This threshold was then applied the time series of daily PRISM precipitation to compute the fraction of precipitation that fell as rain vs. snow.

For all events classified as rain, the tipping bucket data were summarized using the Rainfall Intensity Summarization Tool (RIST), version 3.94 (Agricultural Research Service, USDA, 2015). Rainfall data were divided into fixed intervals at the daily and 5-min time steps, and were also separated into individual storms using a separation threshold of 6hrs of elapsed time with less than 0.5mm of rainfall. RIST outputs included P (cm); storm duration (h); and

maximum 5min and 30min rainfall intensity (cm/h). Using peak 5min rainfall intensity and peak discharge (section 4.4), a lag to peak for each storm was calculated. This lag, calculated in hours, was measured as the time from the peak 5min rainfall intensity to the peak in-stream discharge for the event.

4.2 Snow

Snow monitoring tracked the spatial and temporal patterns of snow in each research catchment. Monitoring consisted of spatial snow surveys and continuous depth monitoring with field cameras and snow sticks, which were demarcated with depth increments.

Snow surveys were conducted at all four watersheds in spring 2015. An initial survey was conducted on 28 February for UT, UI, and BI and on 6 March for BT, due to time constraints. A second survey was conducted at each site on 4 April. Points were collected at 20m intervals along a set transect. Depth measurements were taken with a 1m length of snow depth probe in a 5-point "plus" pattern, with depth taken at a central point and then at 1m distance before, behind, left, and right of this central point (Kashipazha, 2012). Density measurements were also collected at four or more locations along the transects. These density measurements were taken with either (1) a can-o-meter, consisting of two or more size 10 cans (large coffee cans) combined mouth-to-base to form a tube, or (2) a short length (30-40cm) of clear polyvinyl tubing. Samples were measured for depth, using the depth probes, and mass, using AWS digital hanging scales recorded to the nearest gram (American Weigh Scales Incorporated, Norcross, GA, USA). Densities were calculated based on the ratio of mass to volume of the sampling implement. In addition to these measurements, UTM coordinates for

each data collection point, and visual canopy cover descriptions (none [N], open [O], partial [P], or closed [C]) were recorded.

In addition to my own snow surveys in 2015, Ryan Webb monitored snow and soil moisture transects across north/south aspects at each field site. From January 2015 through April 2015, he conducted six surveys of these transects. Each sub-transect was 10m in length, with data collected at 1m intervals. At 1m, 5m, and 10m points, an additional measurement was taken to the right and left of the central survey point, resulting in a total of 17 points collected along each transect (Blumberg, 2012). His observations included snow depth, snow density, and soil volumetric water content (VWC) along each transect. Where applicable, these data have been used to supplement my snow survey measurements.

In addition to the snow surveys, a Stealth Cam Core field camera (Stealth Cam, LLC, Grand Prairie, TX, USA) was deployed at each site. These field cameras were set to take images 5 times each day, hourly from 10am to 2pm. Three snow sticks were placed at a 2-15m distance within the field of view of each camera (Figure 5). These snow sticks were created using a 1.5m length of ¾in PVC pipe demarcated by colored electrical tape at 5cm intervals. Snow sticks were mounted on rebar to keep them upright throughout the season. Camera images were used to determine daily snow depths, with dates recorded for snow on/off and the state of the snowpack (accumulation, ablation, or steady) on a given date. Due to designed snow stick precision of 5cm, observed depths were recorded as either approximately equal to a snow stick depth increment (e.g. ≈5cm) or less than a snow stick depth (e.g. <5cm). An observed value approximately equal to a marked depth increment was rounded to the nearest increment.

Values between marked increments were rounded to a value halfway between two marked increments (e.g 2.5cm, 7.5cm, etc.). A depth of "Trace" was recorded if an amount of snow <5cm in depth and covering ≤50% of the image was observed; these dates were assigned a nominal depth of 1cm.

Figure 5: Peak snow accumulation from the time lapse camera at UT, 18 April 2015; snow sticks are visible in the image.

4.3 Soil moisture and temperature

Soil moisture data were collected at each site using a series of Decagon soil moisture sensors attached to a Decagon Em50 data logger (Decagon Devices Incorporated, Pullman, WA, USA) (Figure 6). Soil moisture was measured at depths of 5cm and 20cm at the upslope and downslope ends of a 10m transect. A Decagon 5TM soil moisture and temperature sensor was

inserted at downslope 5cm depth, and all other sensors were EC-5 sensors recording only soil moisture. In addition to soil moisture, a Decagon ECT air temperature sensor was housed in a radiation shield, co-located with the data logger, and mounted on a 2in PVC pipe at a height of approximately 1m above the ground. All five sensors recorded at a 15-min time step year-round.

Soil moisture data were analyzed by individual monitoring location and as site average values. Site average values were converted to a representative value of soil moisture storage for each site by taking the average volumetric water content value of all four sensors multiplied by 20cm to give a total estimated depth of water stored in the uppermost 20cm of the soil.

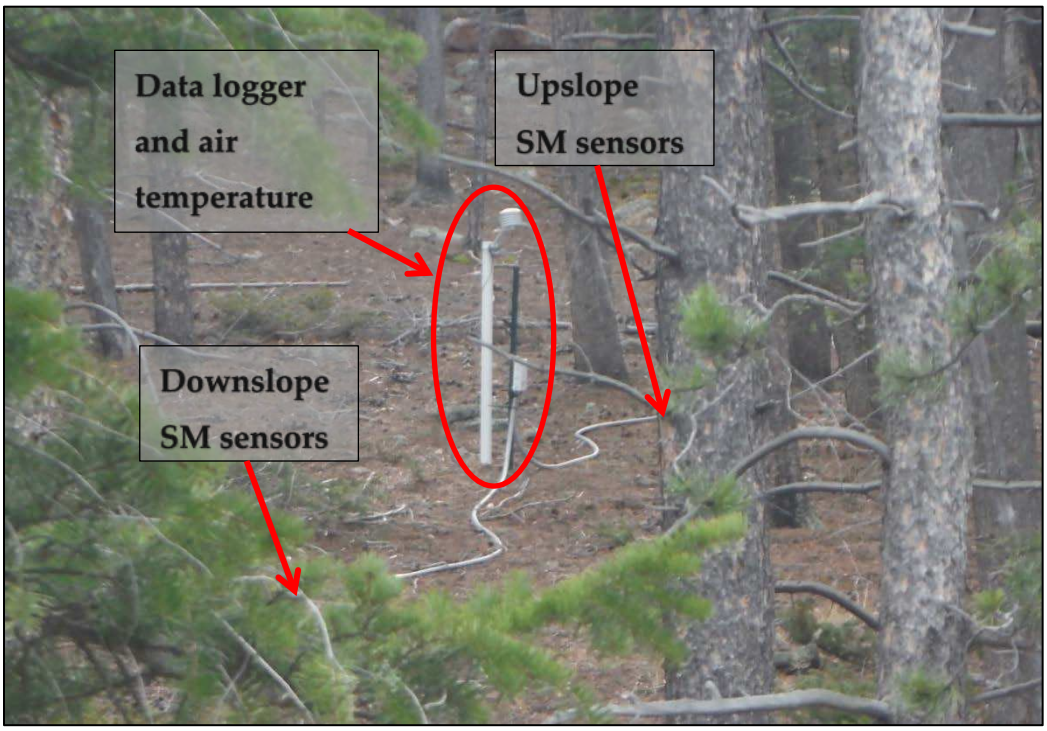

Figure 6: Soil moisture and air temperature sensor locations at UT. Soil moisture sensors are located at 5cm and 20cm depths 5m up- and downslope from the data logger. Air temperature sensor is in radiation shield near data logger.

4.4 Runoff

Runoff was measured in streams draining the outlet of each catchment. Water depth in the channel at all four sites was measured using an In-Situ Rugged TROLL 100 non-vented pressure transducer (In-Situ Incorporated, Fort Collins, CO, USA). Pressure transducers (PT) at UT, UI, and BT were housed within an approximately 1m length of 2in PVC in which dozens of holes were drilled to allow water influx and outflow at different stages (Figure 7a). A hole was augured to bedrock in the stream bed into which the PVC was inserted. The PT was suspended from the top of the PVC with a chain such that the top of the instrument hung level with the streambed surface. Due to a bedrock channel at BI, the PT was inserted into a 20cm length of hole-riddled PVC. This housing was then anchored with a chain to a tree along the stream bank and weighted down with four short lengths of heavy chain to keep it in place. This entire housing was then placed in the stream channel. In order to adjust for barometric pressure in the non-vented PTs, an In-Situ Rugged BaroTROLL was installed at UT and BT (Figure 7b). Barometric pressures recorded at these sites were used to adjust water depth at both the installation site as well as its lower elevation counterpart. In addition to barometric pressure, the BaroTROLL also recorded air temperature. Both the PTs and the BaroTROLLs were set to record continuously at a 5min time interval year-round.

After the barometric pressure correction, some offset adjustments were needed for PT stage values at data download times, as the baseline stage value would sometimes have an apparent shift after extraction of the sensor from its housing during download. The difference between the last valid measurement prior to extraction and the first valid measurement

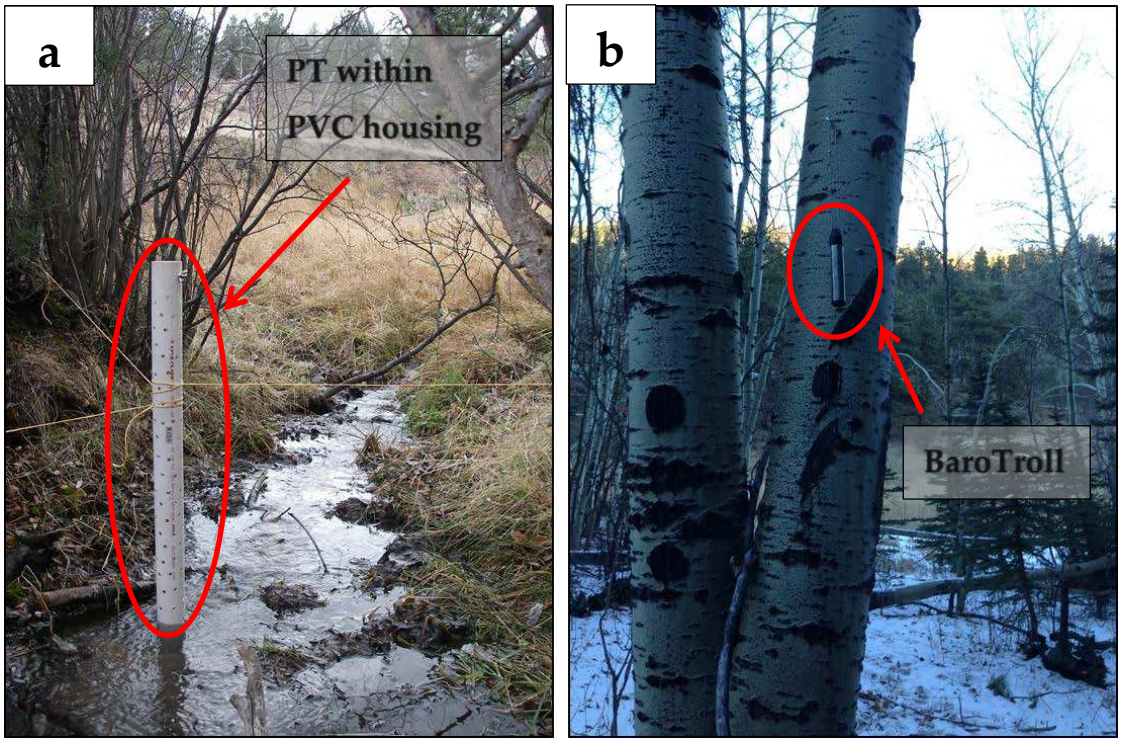

Figure 7: Pressure Transducer (PT) suspended within PVC housing at outlet of study catchment at UI (a), and BaroTroll barometric pressure sensor suspended from an eye bolt near the outlet of the catchment at BT (b).

following reinsertion was applied to all values following reinsertion up to the next download, giving continuity in stage across downloads. This offset-adjusted stage was then put through a 1-D digital filtering function in MATLAB to reduce inherent noise in the data.

During field visits, stage was also manually measured at each site from a fixed point above the stream. A 5m retractable measuring tape was used to measure the distance from the fixed point to both the water surface and the streambed surface. Beginning in May 2015, a staff gauge was added at each site. These staff gauges were attached to lengths of 2x3in wooden board. A steel U-post was driven into the stream bed, and the staff gauge was affixed to this using steel screws. These staff gauges were placed as close to the PTs as possible without

disturbing the streambed adjacent to the PT and where streambed depth allowed for the insertion of the U-post to a depth at which the setup would not wash away.

Both field measurements and Manning equation calculations were used to determine discharge for a given stage. Field discharge measurements were taken using a Decagon ES-2 electrical conductivity and temperature sensor attached to Decagon ProCheck data logger. This sensor was used for salt slug injection stream discharge measurements, as described by Kilpatrick and Cobb (1985). Field discharge measurements did not cover a wide enough range of values for a complete rating curve, so Manning equation discharge calculations were used to supplement these field measurements and create a synthetic rating curve. To develop input data for the Manning equation, stream cross sectional surveys were conducted at each catchment, as described by Arcement and Schneider (1989). Three surveys were conducted at each site, with measurements taken at 5cm intervals across a fixed, level line suspended above the stream from bank to bank. A GPS point with a post-correction horizontal accuracy of 0.1-0.5m was taken at the center of each cross section to determine the slope of the stream between survey points, which were located between 3-5m apart.

Manning's equation follows:

$$V = \left(\frac{k}{n}\right) {R_h}^{2/3} S^{1/2}$$

(Manning, 1889)

where V is velocity in m/s, k is a conversion factor (equal to 1 as all units are SI), n is a derived roughness coefficient, R_h is the hydraulic radius in m derived from the cross section survey, and

S is the slope of the hydraulic grade line in m/m, which was assumed equal to the surveyed channel bed slope. Velocity is multiplied by channel cross sectional area (A) to obtain discharge. To develop a combined field and synthetic rating curve, measured discharge values were plotted against measured stage. Using the cross section survey measurements, R_h and A values were calculated for the stages with measured discharge. These values were used to calculate discharge from the Manning equation, and the value of n was optimized through trial and error so that the equation-derived stage-discharge values matched the observed stage-discharge values. An equation was then fit to the synthetic rating curve, and this curve was applied to to all measured stages to determine discharge throughout WY2015 in liters per second (L/s) (Figure 8). Once discharge was determined in L/s, it was normalized by drainage area to facilitate comparison between catchments. Discharge measurements for comparison in the sections that follow are given in centimeters per day (cm/d).

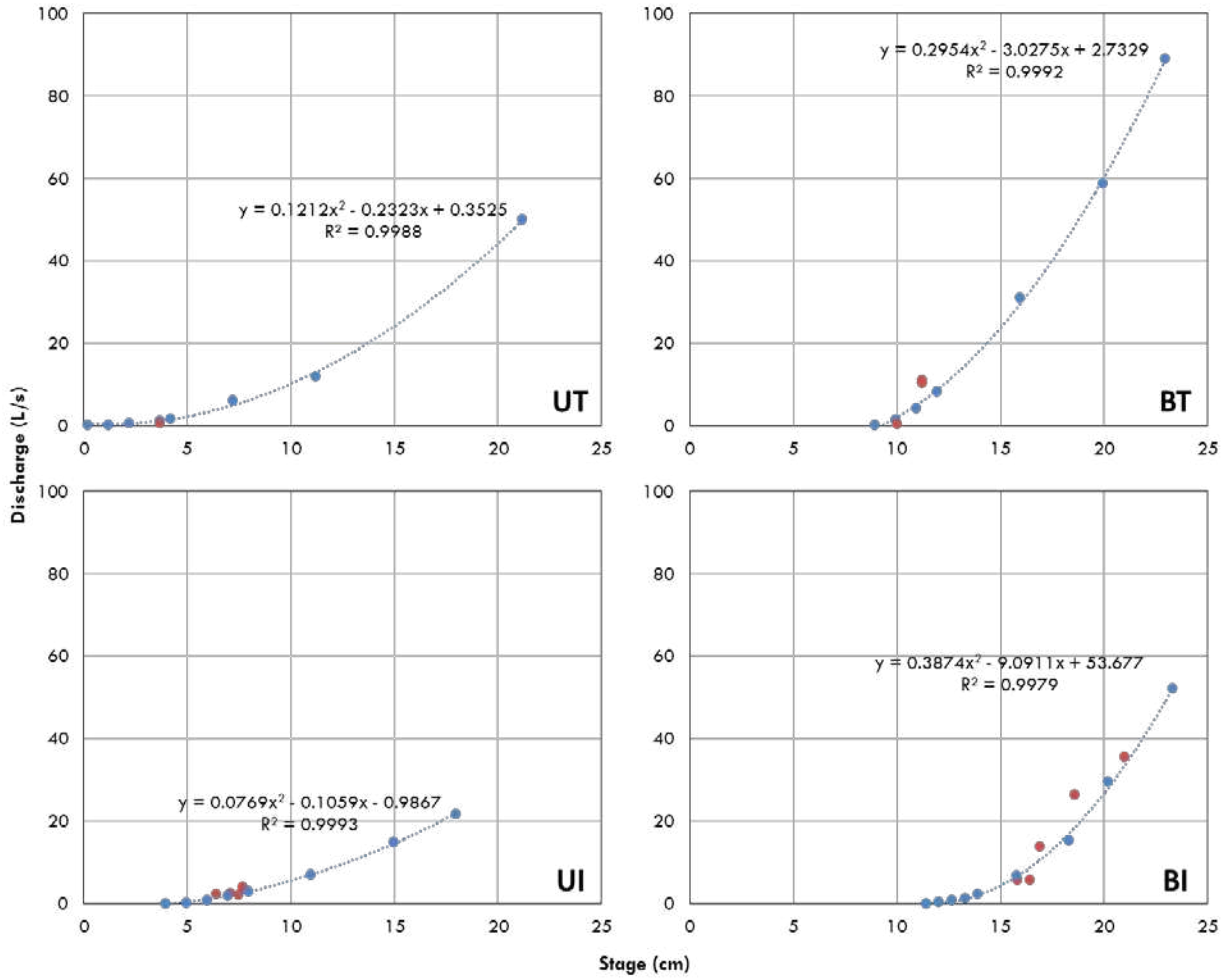

Figure 8: Synthetic rating curves, in blue, with equations and R^2 values for each catchment; red markers show discharge/stage relationships observed in field measurements.

5 RESULTS

Results of this study show how snow, rainfall, soil moisture, temperature, and discharge varied between four catchments in WY2015. To facilitate comparison between the four study catchments, it is necessary to use common units. For this reason, snowmelt, rainfall, soil moisture, and stage will all be given in centimeters to the nearest 0.1cm throughout this section. This varies from the convention of reporting rainfall data in millimeters to the nearest millimeter.

5.1 Snow accumulation and ablation

Time series of snow depth were created for each field site based on field camera observations of snow on/off for the winter and spring of 2014/2015 (Figure 9). These time series chronicle the first snowfall from the beginning of water year (WY) 2015, 1 October, through the final observed ablation of snowpack on 24 May 2015. Snowfall events during this time period can be broadly categorized as three major events (late December 2014, early March 2015, mid-April 2015). Dates of snow surveys are marked on each time series. Significant snow accumulation did not begin at any site until early November. The only major event of the winter months (Dec., Jan., Feb.) came in December. Accumulation began between 14 December and 19 December, with earlier snowfall coming at UT and UI. The greatest amount of winter accumulation came between 24 December and 26 December, with all four sites showing increased accumulation from between 2.5cm – 10cm up to between 22.5cm – 27.5cm. This

represented peak accumulation for this event at UT, UI, and BI. However, peak snowfall at BT lagged slightly behind the other sites, cresting at 32.5cm on 29 December.

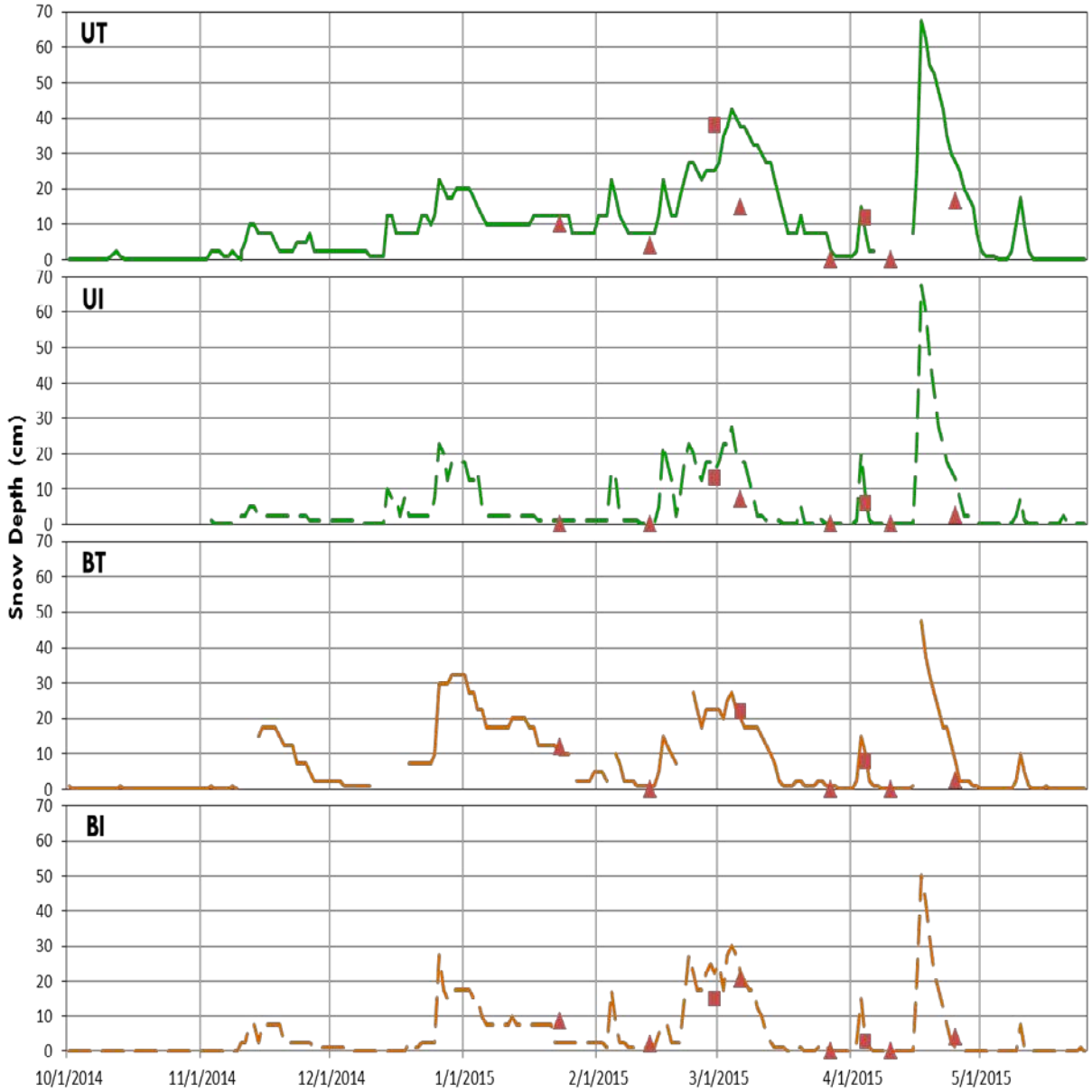

Figure 9: Snow depth time series for UT, UI, BT, and BI for 1 October 2014 to 25 May 2015. Markers indicate snow survey dates (▲ = Webb survey, ■ = Johnson survey) and reflect average snow depth recorded (Webb survey) or snow depth at survey point closest to camera location during the survey on a given date.

Spring months (Mar., Apr., May) brought two major snowfall events, one in early March and another in mid-April. Accumulation for the early March event began around 20 February for all catchments. Accumulation peaked at all sites on 4 March, with snow depth ranging from 25cm to 42.5cm. Ablation occurred rapidly at UI, BT, and BI, going from peak snow depth for the event on 4 March to trace amounts or no snow by 17 March. Ablation also occurred rapidly at UT, though by 17 March snowpack had been reduced only to pre-event depth of 7.5cm. Accumulation for the final major event began on 15 or 16 April at all sites. Snow rapidly accumulated at all four sites, reaching peak accumulation by 17 April. Snow depths ranged from 50cm at BI to peak depths for the event of 67.5cm at both UT and UI. Peak depth at BT was obscured by snow on the camera lens on 17 April, but a depth of 47.5cm on 18 April suggests values higher than this for peak. Complete ablation was achieved between 27 April and 5 May, with final ablation for the event at UT.

Eight snow surveys were conducted at UT, UI, BT, and BI throughout the winter and spring of 2014/2015. Two surveys by Adam Johnson were comprehensive surveys, aiming to characterize snowpack properties across the entire catchment. Six surveys by Ryan Webb were conducted across transects, one at each site, that spanned north and south aspects. Because no single survey coincided with peak depth, all recorded densities were compiled in an effort to characterize density at each site across the snow season. Figure 10 shows that snow density for all sites remained within a range of 118kg/m^3 – 220kg/m^3 for the first seven surveys of the season; the 27 March and 10 April surveys recorded no snow at any site. Higher densities ranging from 282kg/m^3 – 345kg/m^3 were recorded for the 25 April surveying, during the melt

phase of the final major snow event of the season. With the exception of a low density recorded at BT in the 6 March survey, density at burned sites exceeded density at unburned sites on all survey dates. On all dates when snow was present at BI, this site had the highest snow density. By chance, all surveys were conducted during periods of melt or during inter-storm periods, with the exception of the 28 February survey which was conducted during the accumulation phase of the early March major snowfall event.

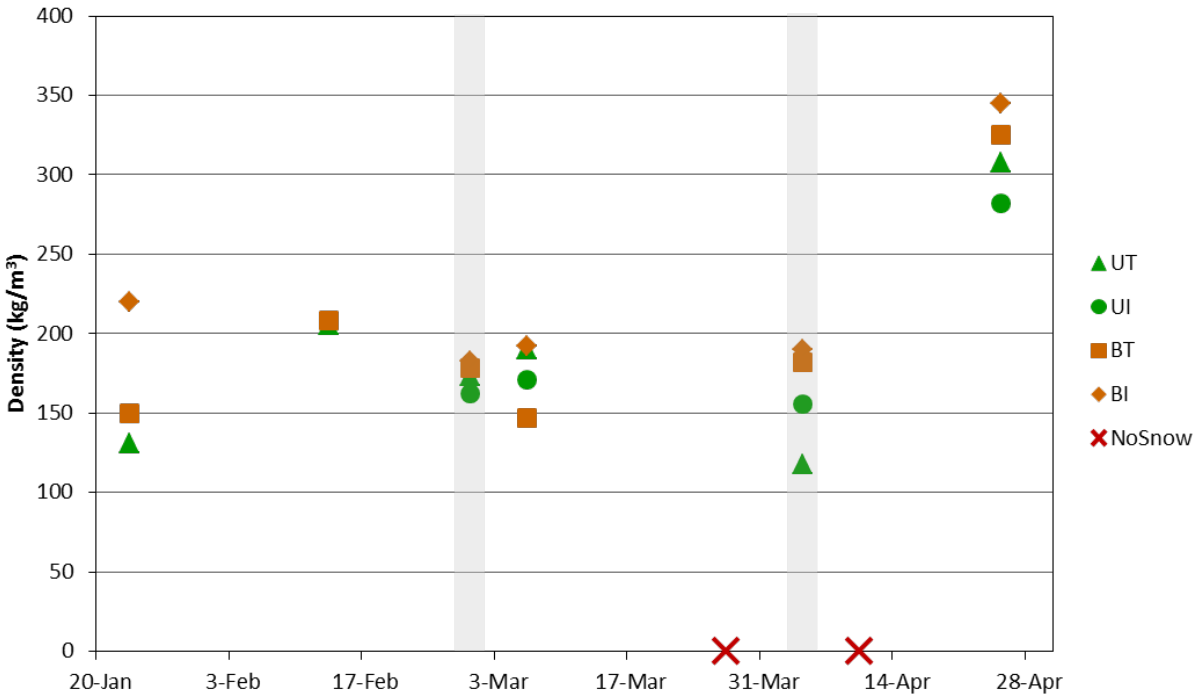

Figure 10: Average snow density by site for each survey conducted by Johnson and Webb between 23 January 2015 and 25 April 2015; Johnson surveys are highlighted in gray; red Xs denote survey dates on which there was no snow present at the survey transects.

Summary statistics for selected snowpack characteristics appear in Table 4. Peak snow depth was higher for both of the unburned sites. These peak snow depths followed a heavy spring snow on 17 April 2015 at all four sites

Table 4: Summary statistics for winter-spring 2014/2015 snow data at all field sites

Site	Total PRISM P as snow, WY2015 (cm)	Peak Snow Depth, observed (cm)[1]	Estimated Peak SWE (cm)[2]	
			Range	**Avg.**
UT	32.0	68	8.0 - 20.9	12.8
UI	29.1	68	10.6 -19.2	13.1
BT	36.4	48	7.1 - 15.6	9.5
BI	26.7	50	9.2 - 17.3	11.3

[1] **peak snow depth taken from field camera observations**

[2] peak SWE given as a range and average based on peak snow depth and densities recorded throughout the snow season during both Johnson and Webb surveys.

Peak SWE values were determined using the following equation:

$$\frac{depth\ (m) x\ density\ (kg/m^3)}{999.8395}$$

The denominator is water density assuming a water temperature of 0˚C. At the time of peak snow depth, no density measurements were collected, so two estimates of peak SWE are provided. First, a range of potential peak SWE values is given using peak snow depth and all densities recorded for each site. Second, an average peak SWE was calculated by averaging all potential peak SWE values returned for each site. These average estimates indicate that SWE accounted for 20% and 23% of peak depth at BT and BI, respectively, and 19% at both UT and UI.

5.2 Precipitation

Precipitation totals for all four catchments were determined from both deployed rain gauges and PRISM simulations. Because it is impossible to separate rain from snow in the totalizing gauges, and undercatch renders total precipitation measured in the totalizing gauges very low for WY2015, PRISM P was used to estimate percentages of rain and snow at each catchment (Table 5). All sites show 10-12% more snow than rain except BI, where 2% more P was rain than snow.

Table 5: PRISM estimates of P for WY2015; percentages of rain and snow reflect PRISM P separated into rain and snow at 2.1˚C mean daily temperature threshold.

Site	Total P, PRISM WY2015 (cm)	% Snow, PRISM	% Rain, PRISM
UT	58.5	55	45
UI	53.0	55	45
BT	64.2	57	43
BI	54.0	49	51

To evaluate the accuracy of precipitation measurements from the field gauges, first rainfall totals were compared between tipping bucket gauges, totalizing gauges, and PRISM estimates at each site. Rainfall totals taken from tipping bucket rain gauges were presumed to be more accurate than snowfall totals from totalizing gauges, though tipping buckets may also undercatch rain. Comparison of TB1 rainfall totals and totalizing gauge rainfall totals from 12 June 2015 through the final totalizing measurement at each site (19 August at UT, BT, BI; 10 September at UI) illustrate the discrepancies between gauges and the issues with undercatch presented by the totalizing rain gauge (Table 6). While there was no pattern based on site

characteristics, a difference of 1-11% between TB1 and the the totalizing gauges was observed at each site, with the totalizing gauges always reporting lower precipitation totals than the tipping buckets. PRISM estimates, however, did show a pattern based on site. Burned site TB1 rainfall totals were similar to PRISM estimates. BT was within 6% of the PRISM estimate, and BI was only site at which PRISM overestimated rainfall, by 10%. Unburned sites showed greater discrepancy between TB1 and PRISM estimates. PRISM greatly underestimated rainfall at both catchments, by a difference of 65-93%.

Table 6: Rainfall totals for TB1, the totalizing gauge, and PRISM estimate for all four catchments, as well as % differences from TB1 measured rainfall; all totals begin on 12 June 2015 and end on 18 August 2015 for UT, UI, and BT and 9 September 2015 for BI.

Site	TB1 (cm)	Totalizing (cm)	PRISM (cm)	% difference, TB1_Totalizing	% difference, TB1_PRISM
UT	22.3	20.5	11.5	8	93
UI	18.0	16.2	10.9	11	65
BT	14.1	12.6	13.3	11	6
BI	10.9	10.8	12.1	1	-10

Because of discrepancies between the two precipitation gauges and the PRISM estimates, total input to the system from rain and snowmelt was also determined using the snow depth data and measured snowpack densities for each catchment. For each day with loss of snow depth in the camera, water input from snowmelt was converted from snow depth to snow water equivalent using a minimum, maximum, and mean value of snow density. These depths of snowmelt as snow water equivalent were added to the rainfall totals from the tipping buckets at each site to compute the total water year (WY) input. Table 7 compares these field-derived values of total WY input to total WY precipitation from PRISM. This comparison

shows that PRISM was underestimating precipitation, though the magnitude of this underestimation was dependent on the density used to determine SWE. PRISM underestimated input under all scenarios, by an amount ranging from 5-45%.

Table 7: Comparison of PRISM estimates of input for WY2015 to measured and computed inputs from snow camera observations and tipping bucket data at all four catchments.

Site	PRISM input (cm)	Snow density (g/cm³)		Input (cm)	% diff
UT	58.5	Min	0.12	61.7	5
		Max	0.31	104.3	44
		Mean	0.19	77.4	24
UI	53.0	Min	0.16	66.0	20
		Max	0.28	95.1	44
		Mean	0.19	74.6	29
BT	64.2	Min	0.14	68.3	6
		Max	0.33	104.4	38
		Mean	0.20	78.6	18
BI	54.0	Min	0.18	67.5	20
		Max	0.35	98.9	45
		Mean	0.23	75.9	29

5.2.1 Rainfall depth

Rainfall from TB1 in each catchment is shown in Figure 11. The transition from primarily rain to primarily snow occurred in mid-May, but some rainfall was evident during winter months based on temperature thresholds and camera data. The three major rainfall events of WY2015 are highlighted in the gray boxes along with total cumulative rainfall for the event. P and Cumulative P are shown in daily time steps in Figure 11.

Periods of rainfall throughout the summer were similar at all four catchments, though magnitude and intensity of daily rainfall varied. Three major periods of persistent rainfall are evident in Figure 7: mid-May, early July, and mid-August. These three events account for the greatest contributions to cumulative P. The mid-May event occurred immediately after final ablation of the snowpack at all four sites. This period of rainfall was shorter and of lesser magnitude at UT and UI than at BT and BI. The mid-May event accounted for 8-28% of total summer rainfall in each catchment. Rainfall totals for the event ranged from 2.5-8.0cm. The early July rainfall event had a similar duration at all sites, lasting 15-17 days, but was of a much greater magnitude at UT and UI than at BT or BI. This event accounted for 24-39% of total seasonal rainfall in each catchment. The mid-August event also had a similar duration at all four catchments: 7 days at UT, UI, and BT, and 6 days at BI. Magnitude of this event was again higher at UT and UI. The mid-August event accounted for 8-14% of total summer rainfall at each site. Overall, these three events accounted for 58-60% of all recorded rain fall at each site.

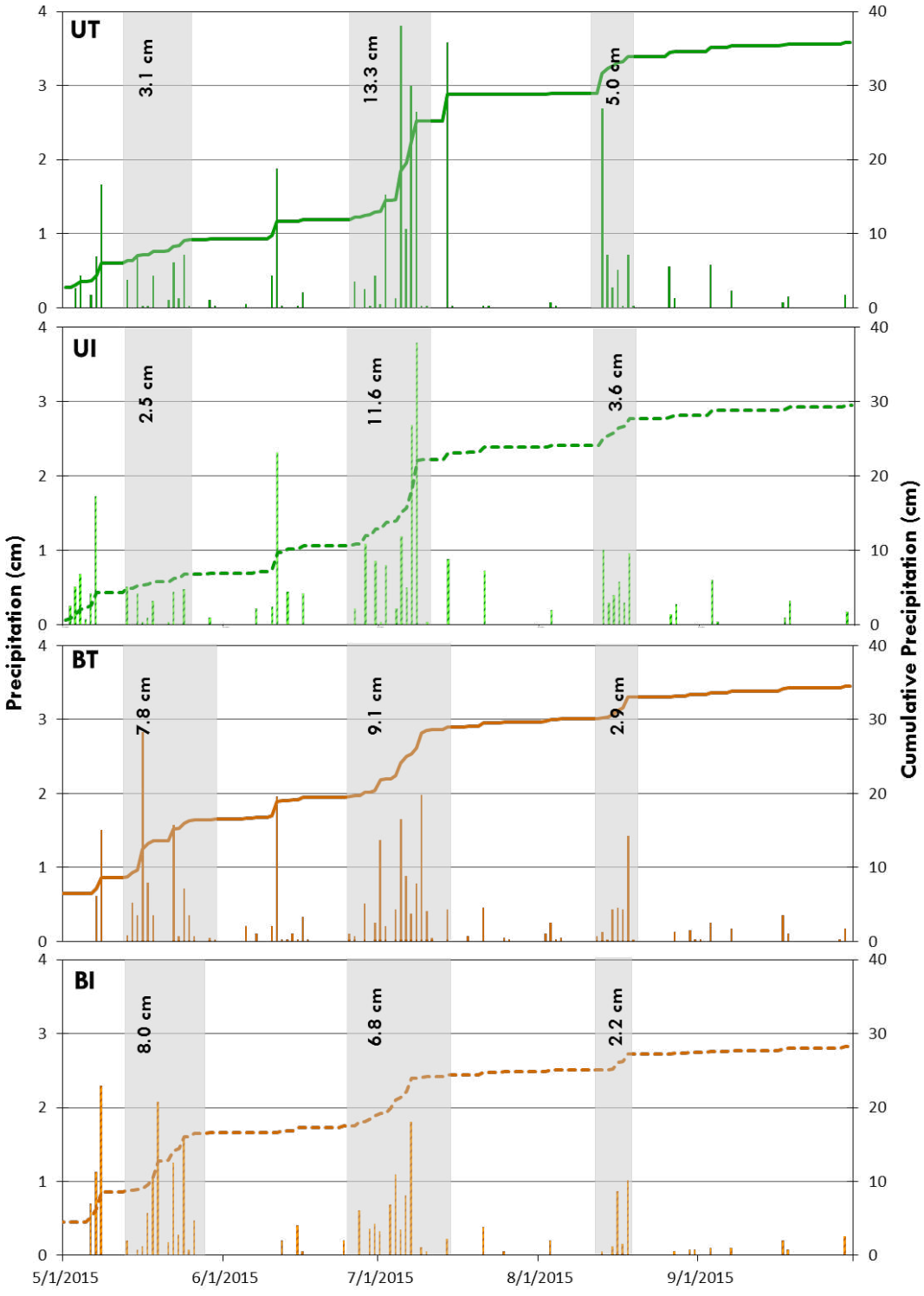

Figure 11: Daily rainfall and cumulative rainfall for 1 May 2015 through 30 September 2015 at all catchments; totals derived from TB1 at all sites; major periods of persistent rainfall are highlighted in gray boxes with rainfall totals; box widths vary based on duration of rainfall.

5.2.2 Rainfall intensity

Examination of rainfall intensity focused on events with a 30-min intensity (I_{30}) of 1cm/h or greater, a recognized threshold for runoff production following wildfire in this region (Moody & Martin, 2001). Table 8 shows summary statistics for all storms surpassing this I_{30} threshold. Many more storms surpassing this threshold occurred at unburned sites than at burned sites in WY2015, highlighting differences in weather patterns between the catchments. At unburned catchments, most storms were recorded at both catchments with the exceptions of 30 June, 8 July, and 21 July storms that occurred only at UI and 14 August and 26 August storms that only occurred at UT. Rainfall was recorded at both catchments on all of these dates, but the I_{30} threshold required for inclusion here was not surpassed. Both storms at the burned catchments that surpassed the intensity threshold occurred on the same dates.

Average storm duration was much greater at unburned sites than burned sites. However, this number is inflated by the large number of longer duration, cyclonic storms recorded at unburned sites during the early summer months. The convective storms that were recorded at all four catchments in late summer were shorter in duration. Often, long duration storm profiles were dominated by long periods of low intensity rainfall interspersed once or multiple times with bursts of high intensity rainfall which surpassed the I_{30} threshold. High intensity rainfall was almost always correlated with a rapid rise to peak in discharge, even for longer duration storms. The average lag to peak discharge was greater for unburned catchments than for burned catchments, though this was due to two storms at UT and three at UI that had much longer lags than other storms (Table 8). The dearth of high intensity storms

experienced by burned sites made a direct comparison of lag times between unburned and burned catchments difficult.

Table 8: Total rainfall from TB1 and summary statistics for all rainfall events exceeding an I_{30} threshold of 1.0cm/h

Site	Total Rain, TB1 (cm)	Events with I_{30} > 1.0cm/h	Avg. event I_{30} (cm/h)	Avg. event I_5 (cm/h)	Avg. duration (h)	Avg. lag to peak (h)
UT	35.8	11	2.5	7.0	5.1	0.8
UI	29.4	14	1.5	4.5	7.5	1.1
BT	34.5	2	1.8	5.7	0.7	0.6
BI	24.3	3	1.3	4.3	0.6	0.2

5.3 Air and soil temperature

Air and soil temperature variability was similar across all four catchments, regardless of burn status or snow zone. As might be expected, air temperature showed much greater variability day to day than soil temperature (Figure 12). All catchments had a period of higher air and soil temperatures in October and November, slowly declining as the year progressed. Winter soil temperature stayed close to 0˚C while air temperature reached as low as -26˚C. Spring brought steady increases in both soil and air temperatures, with soil temperatures showing variability more similar to air temperature as snowmelt began in earnest. During summer months soil temperatures were relatively stable, between 12-20˚C. Air temperature during summer months was also high but showed some correlation with major rainfall events, with storm systems bringing drops in air temperature for the July and August rains.

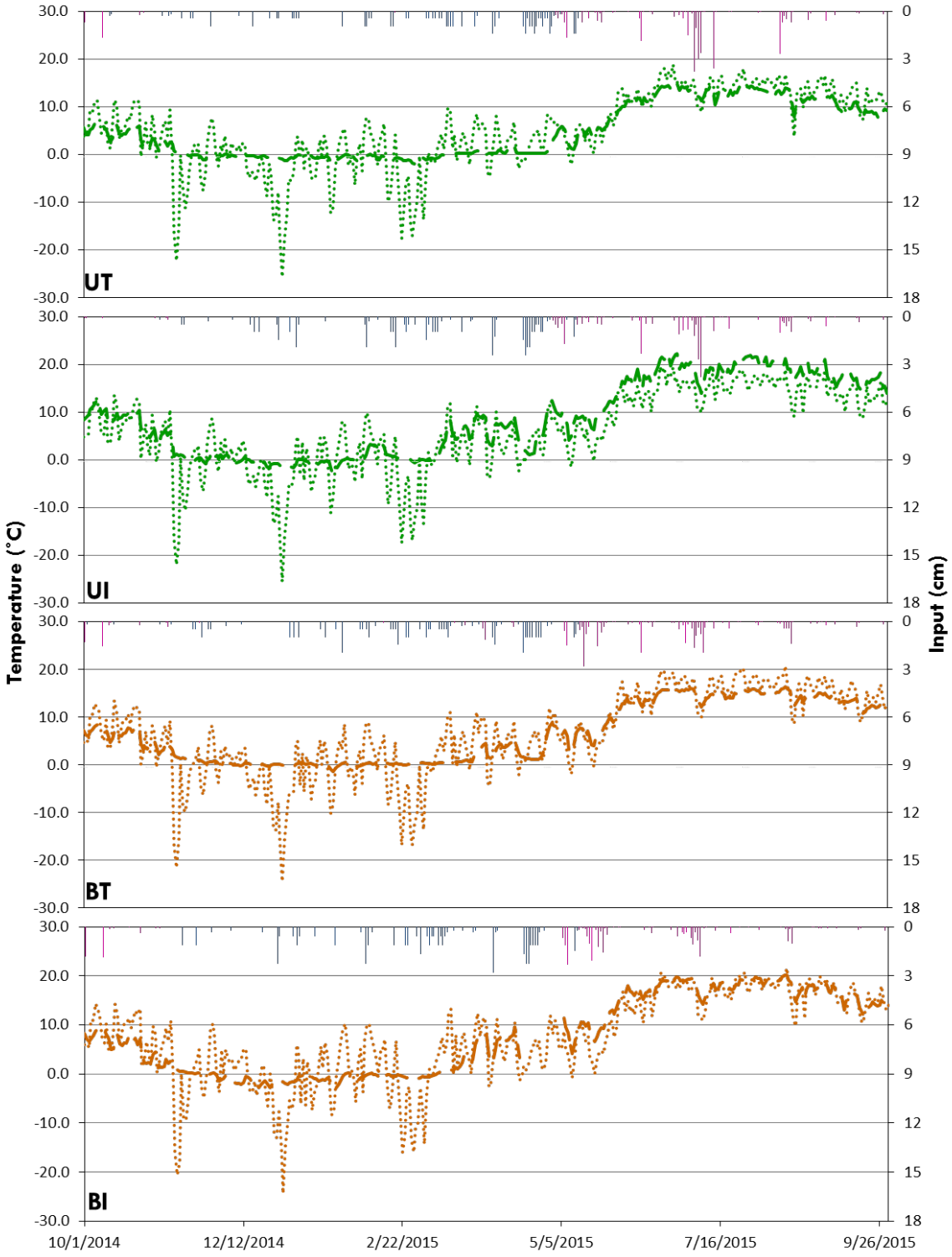

Figure 12: Air (dotted) and soil (dashed) temperature for all catchments and daily snowmelt (blue) and rainfall (pink) input; mean snow density was used to compute snowmelt input.

While all four catchments were generally similar in patterns of air and soil temperature, there are some notable similarities and variations between sites (Table 9). Soil temperatures at UT remained stable at near 0˚C well into late April, due to the deeper and more persistent snowpack. All other sites showed notable increases of 3-5˚C in soil temperature in mid to late March. The persistent snowpack at UT also resulted in less variation in soil temperature during the rise toward summer conditions. Summer soil temperatures were higher at ISZ catchments than at TSZ catchments. Air temperature was remarkably similar in pattern at all four catchments. However, annual air temperature averages show a gradation in temperature with elevation, moving from an annual average of 4.9˚C at UT to 7.2˚C at BI. Burned catchments had higher annual average air temperatures than their unburned counterparts (Table 9). Soil temperatures, however, were separated along snow zones rather than fire effect. Burned and unburned TSZ catchments had very little difference in their mean soil temperature and mean air temperature. At ISZ catchments, however, mean soil temperature was higher by 5-30% at the corresponding unburned site.

Table 9: Summary statistics for air and soil temperature at all catchments. Values are averages for WY2015.

Site	Daily air temperature (˚C)			Daily soil temperature (˚C)		
	Min	Max	Mean	Min	Max	Mean
UT	-25.7	18.8	4.9	-2.1	15.2	4.6
UI	-25.5	19.6	6.1	-3.2	22.3	8.7
BT	-24.6	20.7	6.3	-1.5	16.3	6.3
BI	-24.3	21.6	7.2	-3.3	20.1	7.6

5.4 Soil moisture response

Soil moisture response showed clear variability between burned and unburned monitoring sites in the uppermost 20cm of the soil column, but seasonal patterns were similar for all sites (Figure 13). Soil moisture was high in October and November, before the first snowfall of the year. Beginning in mid-November, soil moisture dropped, coinciding with the beginning of seasonal snowpack. Some muted responses are evident to melt events associated with unseasonably warm temperatures in January and February. Low values persisted until mid-March, when early spring snowmelt events increased soil moisture. Soil moisture rose to highest annual values through April and May, fluctuating with spring snow storm accumulation and ablation. Peaks in soil moisture were associated with ablation events in late March, early April, late April, and early May. The highest annual inputs occurred during these spring ablation events. As meltwater gave way to summer rainfall dominance in mid-May, soil moisture values rose to annual maxima due to heavy rainfall on soils already wet from meltwater inputs from the final snow ablation of the spring. Soil moisture declined through the summer, with the exception of three increases in moisture from rain events in June, July, and August. Following the final major rainfall event, soil moisture steadily declined, ending WY2015 with lower overall stored soil moisture than at any other time annually.

Taken as a site-by-site comparison, patterns in soil moisture increase and decrease reveal substantial differences between the monitoring locations in burned and unburned catchments and between transitional and intermittent snow zones. Soil moisture storage at BT and BI was 34-43% higher at the beginning of WY2015 than storage at UT and UI. Soil moisture was also

higher at TSZ sites than at ISZ sites by 5-9% at the beginning of WY2015. During the winter seasonal low, burned sites had 30-52% higher storage than unburned sites, and TSZ sites had 8-26% less stored soil moisture at their lowest than ISZ counterparts.

Peak soil moisture following snowmelt also varied between monitoring locations. BI reached a recorded peak first on 18 April at 7.2cm, higher than soil moisture recorded at any other catchment by at least 20%. BT peaked on 26 April at 6.6cm, equaling peaks later in the month of May. UT peaked last, on 29 April at 4.2cm, due to the most persistent snowpack of any catchment. All sites reached a low in soil moisture storage on 10 June before rainfall events across all four catchments between 10 June and 16 June caused a rapid increase in soil moisture storage. The magnitude of this increase was much greater at unburned sites than at burned sites, with increases of 15 – 43% at UT and UI compared to 6 – 7% at BT and BI. A steady decline followed this minor peak, with all sites reaching early summer lows between 27 June and 1 July. The heaviest rainfall of the summer began across all four catchments between 28 June and 10 July resulting in peak soil moisture values for the summer at all sites except BT. UI continued to experience the greatest variability and had the lowest soil moisture at all sites throughout the rest of the summer save three days in August when it briefly surpassed BT. On 29 July, soil moisture storage at BT and BI dropped below storage at UT for the first time all year. Storage at UT would remain the highest at any catchment for the rest of WY2015. A final major rainfall event of the summer resulted in a mid-August peak, though variability in the timing of rainfall across catchments changed the timing of the soil moisture spike. Following

the final major rainfall event, all sites steadily declined and all sites finished WY2015 with 31-76% lower storage than they had at the beginning of the water year.

Overall, soil moisture storage was higher throughout most of the year at burned catchments than at unburned sites, but prolonged periods of dry weather in the late summer brought soil moisture storage at burned catchments below soil moisture storage at UT. Annual peaks for all sites except UT occurred during snowmelt, highlighting the importance and dominance of snowmelt in this region. Steady snowmelt inputs raised soil moisture storage to high levels and maintained them there, while episodic rainfall input caused soil moisture to rise rapidly, peak, and recede quickly.

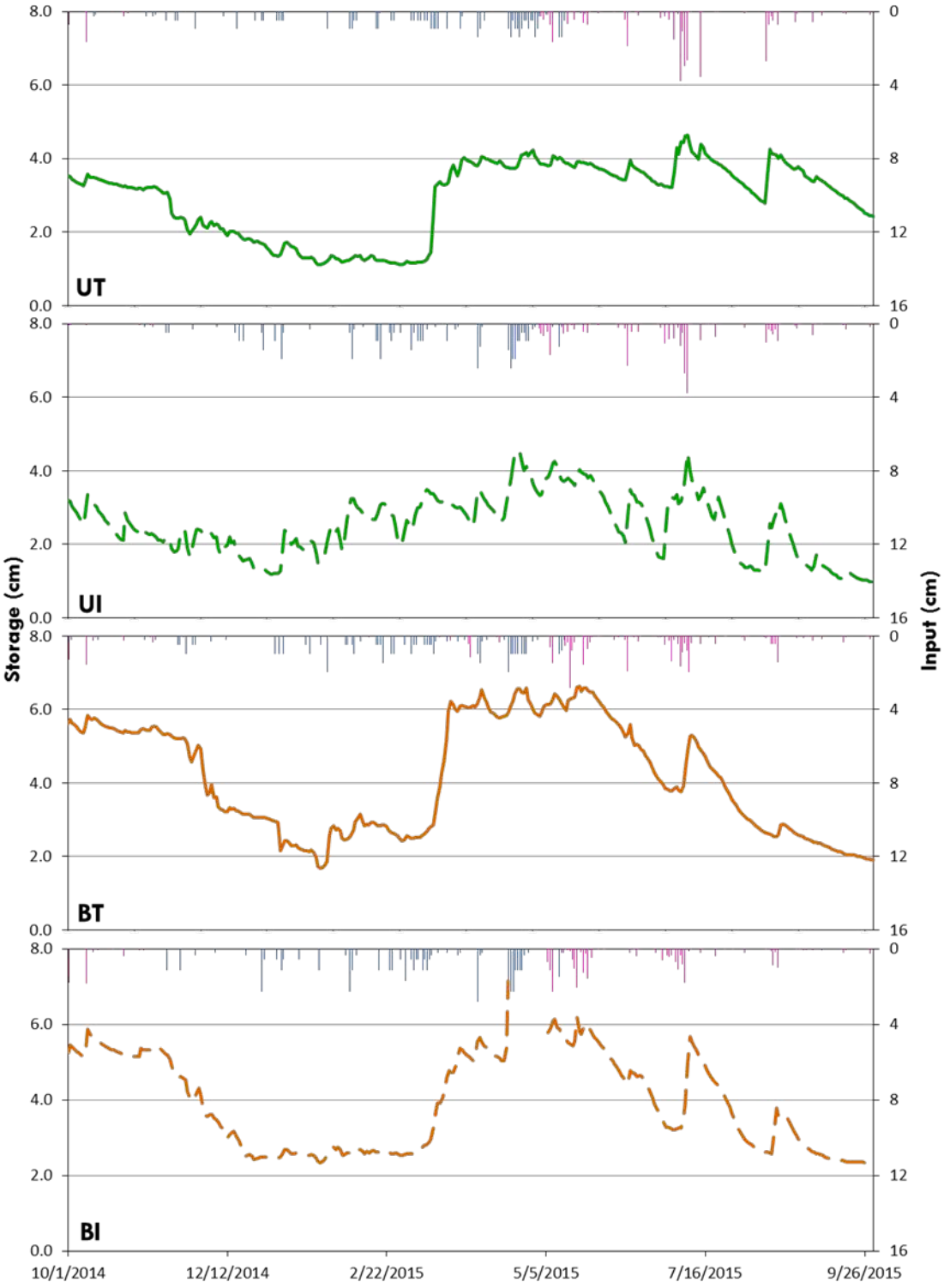

Figure 13: Soil moisture storage in the uppermost 20cm of soil at each catchment with daily snowmelt (blue) and rainfall (pink) inputs; mean snow density was used to compute snowmelt input.

5.5 Runoff

Discharge at all sites remained low throughout the early part of WY2015. Lack of winter discharge measurements led to reliance on synthetic discharge rating curves created using discharge measurements and channel profiles taken during summer months (Figure 8). Field observations of stream conditions at all four catchments during winter months suggest that ice in the streams and lack of input from snowmelt kept discharge low. Discharge increased in spring, and this increase began earlier at burned sites than unburned sites, with BT and BI seeing increased discharge due to snowmelt in early April while UT and UI did not begin to have increased discharge until late April (Figure 14). At all sites snowmelt was immediately followed by May rainfall, leading to mixed rainfall and snowmelt runoff sources for the hydrogaph peaks in May. A dry period in early June led to decreased discharge. All sites had a summer peak in discharge occurred in July following heavy rainfall, but this peak was lower than the spring peak except at UI and more prominent at TSZ sites than at ISZ sites. Following this July peak, all sites experienced steady decrease in discharge throughout the rest of the summer despite heavy rain in mid-August.

Site by site comparison reveals greater complexity in discharge patterns (Figure 14). Discharge at UI and BT was negligible throughout the winter months, from October through mid-April. Winter discharge at UT and BI was more variable. BI showed the greatest variability through the winter months. Following the large snowmelt in mid-April, both BT and BI showed peaks in discharge, with BI peaking first. Neither UT nor UI showed a peak hydrograph response for the mid-April event. UT discharge continued to rise steadily until the

second week of May, due to a deeper, more persistent snowpack and a larger early May snow accumulation than any other site. UT did not peak until 10 May, when a combination of snowmelt and rainfall resulted in the highest annual peak discharge for all catchments at 0.69cm/d. The snowmelt and rainfall combination in May also produced the annual peak flow at BY. The intermittent catchments experienced peak flows either earlier in the season during snowmelt (BI) or later in season after the July rains (UI).

23 April was chosen as a point of separation in discharge from frozen conditions to snowmelt because it is the date of the initial peak in discharge at any site, in this case BI. Using 23 April as a demarcation date, all catchments experienced the majority of their discharge in the latter half of WY2015. At UT, UI, and BT, discharge after 23 April represented 89 – 99% of discharge. BI, however, experienced a smaller percentage of discharge after 23 April, 56%. Discounting discharge before 23 April, TSZ catchments had much higher average discharge than ISZ catchments, by 92% at unburned catchments and 19% at burned catchments. Considering the entire water year, however, UT still has a much higher average than UI, still 92%, but average discharge at BI surpasses average discharge at BT by 33%.

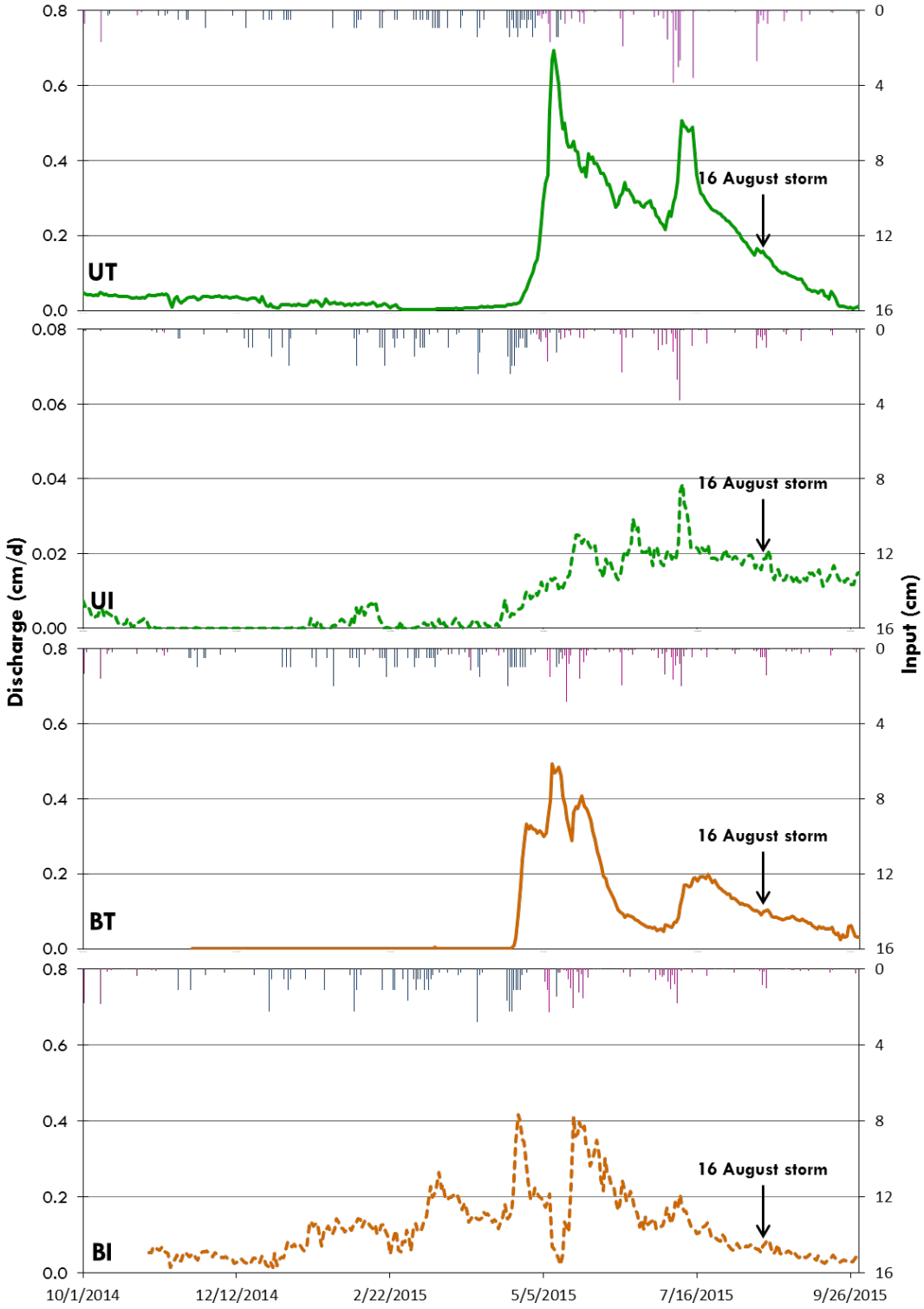

Figure 14: Time series of discharge normalized for catchment area and cumulative snowmelt (blue) and rainfall (pink) input for all catchments. Y-axis for UI is one order of magnitude smaller than other y-axes to highlight seasonal variability at the catchment; mean snow density was used to compute snowmelt input.

Although the dominant signal in all hydrographs is the seasonal snowmelt response, runoff from rainfall events also caused some hydrograph response, as evident in the increased discharge at all sites following the July rains. All sites experienced high intensity rainfall events during summer months that exceeded a 1.0cm/h I_{30}, though variability in weather patterns meant that few of these high intensity storms were experienced at all catchments during the same storm (Table 8). The only storm that exceeded the 1.0cm/h runoff production threshold at all catchments was on 16 August (Figure 15). This storm was a high-intensity convective storm, with I_{30} values ranging from 1-1.7cm/h. Duration was similar at all sites, 0.3-0.6h, and total rainfall for the event was also similar at all sites, 0.5-0.9cm. UT, BT, and BI experienced similar peak discharges within 0.2-0.4h after peak precipitation, indicating IEOF at all sites. UI, always the least responsive of the streams, had a lower peak. The magnitude of change in discharge was greater at burned catchments than at unburned catchments. Baseflows of approximately 0.05-0.08cm/d at burned catchments increased to peaks of 0.14-0.16cm/d. In contrast, baseflow of approximately 0.15cm/d at UT increased to a peak discharge of 0.19, 50-66% less of a change in magnitude than burned counterparts. Here again, the increase in discharge at UI was considerably less. BI reached peak discharge 0.2-0.3h faster than other catchments, thanks to both the highest I_{30} value and the greatest total rainfall for the event.

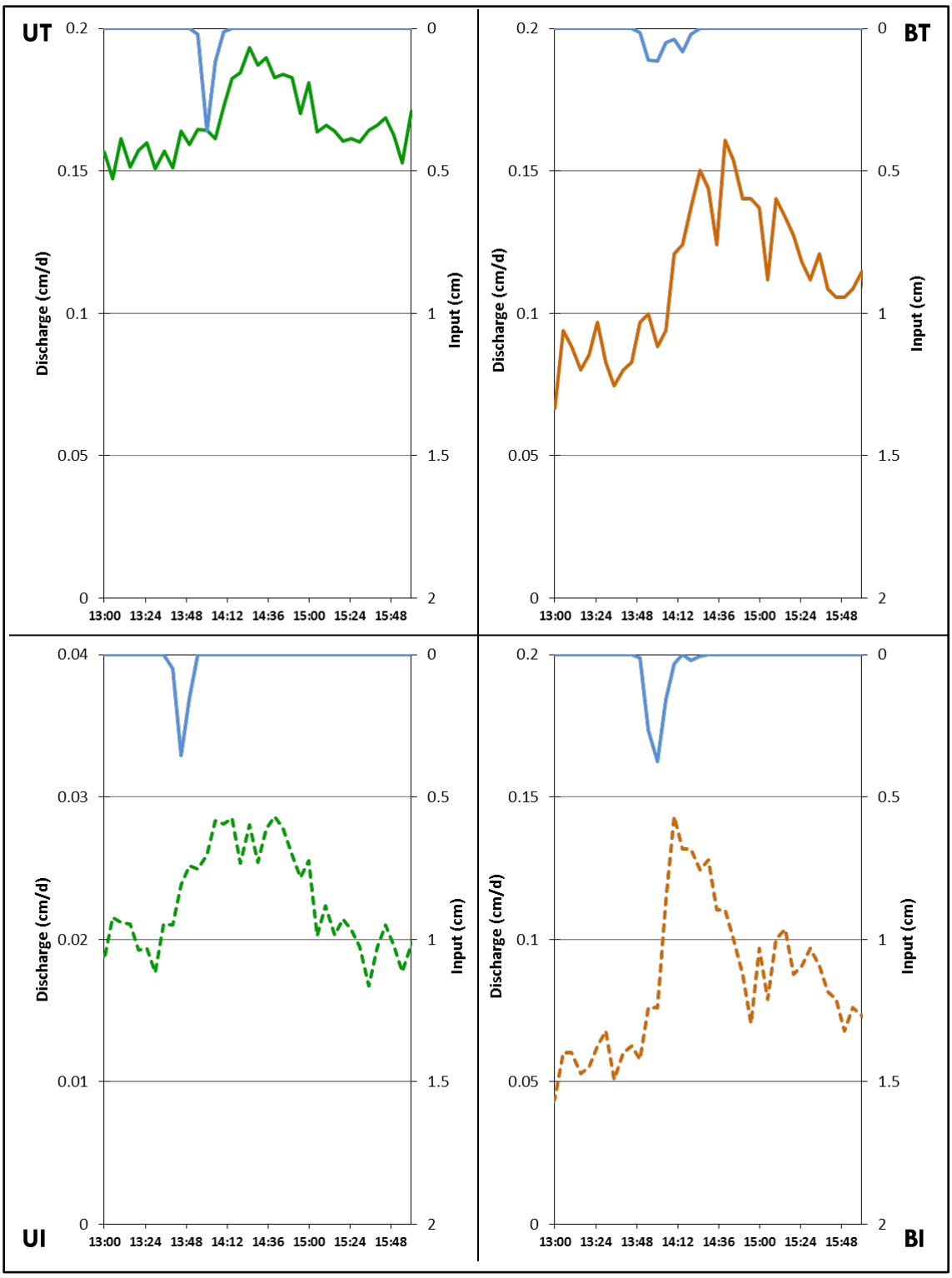

Figure 15: Storm hydrograph and input hyetograph for rainfall event on 16 August 2015; discharge for UI is a smaller increment to highlight variability in hydrograph; x-axis runs from 13:00 to 16:00 to highlight the storm event. Rainfall data from TB1.

5.6 Synthesis of variables

For input variables, peak snow depth was higher at unburned catchments than at burned catchments (Table 10; Figure 16); however this may have been due to a greater amount of snowfall during the mid-April snow event during which peak depths were recorded. Both snow density and annual mean air temperature were higher at burned catchments than their unburned counterparts. Air temperature was also higher in intermittent than transitional sites. Rainfall was higher at unburned catchments. In spite of spatial variability in storm patterns across these catchments, total input of rainfall and snowmelt was similar at all catchments, with variability no greater than 5%. Snowmelt dominance of the hydrologic regime at these catchments is supported by 71-86% of total input coming from snowmelt. The snowmelt contribution to input was greater at ISZ sites than TSZ sites.

For response variables, soil moisture storage was higher on average at burned catchments and higher in transitional than in intermittent catchments. Average soil temperature showed no evident relation to burn status but was higher at ISZ catchments than at TSZ catchments. Discharge as a ratio of input (Q/Input) highlights the variability in the amount of input from each catchment that was removed via runoff and stream discharge. Q represented 33-55% of input at UT, BT, and BI. UI was remarkably lower in discharge, with only 4% of input accounted for in measured discharge. Total Q was highest at UT and BI, 93% and 34% higher, respectively, than their wildfire-effect counterparts. Both sites had similar Q/Input values despite being located at opposite extremes of the elevation-burn matrix.

Table 10: Summary of input and response variables for all four catchments. Values are averages for WY2015.

Variable		UT	UI	BT	BI
Snow	Peak depth (cm)	68	68	48	50
	Mean density (g/cm^3)	0.19	0.19	0.20	0.23
Rain (cm)[1]		22.3	18.0	14.1	10.9
Input (cm)[2]		77.4	74.6	78.6	75.9
Storage (cm)[3]	Mean	2.9	2.5	4.1	3.9
Air temperature (˚C)	Mean	4.9	6.1	6.3	7.2
Soil temperature (˚C)[4]	Mean	4.6	8.7	6.3	7.6
Discharge (cm/d)		42.8	3.0	25.5	38.6
Q/Input (%)		55	4	33	51

[1]Rain total represents measurements from TB1

[2]Input is the sum of snowmelt derived from mean snow density and TB1 rainfall

[3]Storage represents soil moisture in the uppermost 20cm of soil at each catchment

[4]Soil temperature taken at 5cm depth at each catchment

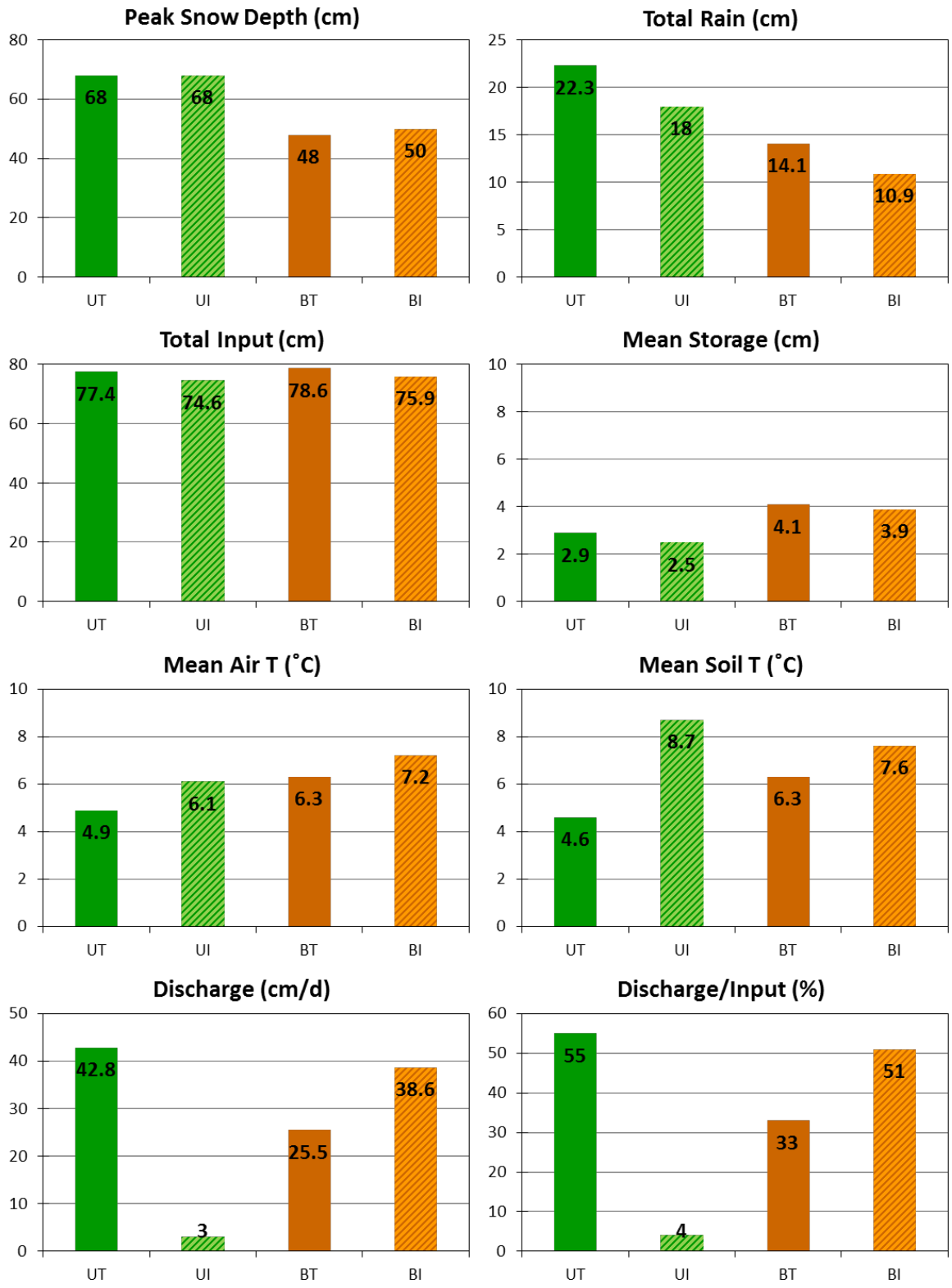

Figure 16: Graphical representation of summary statistics from Table 10.

6 DISCUSSION

This research highlights the complex processes that affect how wildfire impacts the timing and magnitude of runoff generation in the study area. Comparison of these catchments highlights differences in the hydrologic regimes of the catchments and begins to answer a number of interesting questions about how weather patterns, elevation, and land cover may affect hydrologic responses in this region.

6.1 Snow

Based on prior research (e.g. Burles and Boone, 2011), it was expected that burned sites would experience greater snow accumulation and more rapid ablation than unburned sites because removal of canopy cover decreases interception and subsequent sublimation of snowfall while also allowing for increased solar insolation to ablate the snowpack. However, snowpack at all catchments showed similar patterns in timing and magnitude. Dates of accumulation and ablation are temporally similar at all sites, suggesting that the same winter storms produced snow at all sites. Winter air and soil temperatures are also very similar at all sites. These similarities in snowfall timing and soil temperature contrast with the expectation of later snow accumulation and more variable soil temperature at burned sites (Molotch et al., 2009). However, despite these similarities, the snowpack at burned sites was consistently denser than the snowpack at unburned sites. A denser snowpack may result in increased SWE as meltwater accumulates within the snowpack itself. This denser snowpack may be the result of increased solar radiation at burned sites, as observed by Burles and Boon (2011). The fact

that all surveys, with the exception of the 28 February survey, were conducted during melt periods supports this possibility. However, neither solar radiation nor the density of initial snowfall data were collected at the monitoring sites; these data would have been useful to determine what caused the differences in measured snow density between sites.

Because of the position of these sites near the intermittent-persistent snow transition, they did not accumulate snow consistently throughout the winter and spring and instead had several periods of mid-winter accumulation and ablation. This means that peak snow depth and SWE differences were functions of event-specific differences in snowfall or snowmelt rather than the cumulative effects over an entire snow season. Due to the dominant influence of a single snow event on peak SWE, results of this study do not illustrate a clear effect of burn conditions on snow accumulation. This problem could be remedied by increasing sampling locations to include a greater number of adjacent burned and unburned areas, effectively reducing the spatial variability in snowfall.

Another anticipated outcome of this research was that the snowpack would be more persistent at TSZ catchments than at ISZ catchments. This expectation was met in unburned sites but not burned sites. UT showed a persistent snowpack throughout the winter months, with no complete ablation of the snowpack until April (Figure 9). All other catchments, including BT, experienced periodic total ablation of the snowpack throughout the winter months. The timing of ablation was consistent across UI, BT, and BI. This suggests the possibility that the removal of canopy cover and resulting increase in solar insolation following wildfire observed in other studies (e.g. Harpold et al., 2014; Burles and Boon, 2011) may have

caused BT to experience more rapid ablation than it did prior to the fire. Snow persistence mapping used to select catchment location used pre-fire snow cover data (Moore et al., 2015), suggesting that the snow persistence at BT was higher before the fire.

Catchment aspect may also play some role in retention of snowpack, especially in the comparison of UT and BT (Figure 2). BT is the only catchment with a northeastern aspect. All other factors being equal, it is reasonable to expect that BT would retain snowpack better than UT, which has a southwestern aspect. Here again, this was not the case, another indication of a burn effect on snow persistence at BT. The effects of BT being burned, though, may or may not be the primary culprits, as BT also had different weather patterns and a shallower, denser snowpack. Furthermore, the limited scope of monitoring may also be affecting interpretation of conditions at each catchment. All catchments encompass a variety of canopy, aspect, and slope conditions, which may not be fully accounted for by snow surveys and monitoring sites. Data taken from monitoring locations may not fully represent the range of catchment-wide variability.

6.2 Rain

Patterns and magnitude of rainfall were quite dissimilar between burned and unburned catchments. Unburned catchments experienced storms of greater magnitude and intensity throughout summer months than burned catchments, though timing of rainfall events was similar. Schmeer (2014) also found comparable levels of heterogeneity in summer storm magnitudes while working in the High Park Fire area; other studies have likewise reported rainfall variability in mountainous regions (Osborne et al., 1972; Linderson, 2003; Smith et al.,

2014). This difference in weather patterns makes comparison of the rainfall responses between the burned and unburned sites difficult, and there was only one high intensity storm that affected all four catchments. For this 16 August storm, burned catchments exhibited an increase in discharge of a greater magnitude than unburned sites. This may have to do with differences in infiltrability of soils, as suggested by Moody and Ebel (2014), with lower infiltration rates in the burned areas. However, this study was conducted three years after the fire, and substantial vegetation and infiltration recovery (Schmeer, 2014) has reduced the differences between the soil properties of burned and unburned catchments. Other burned catchments in this study region had higher intensity rains during the 16 August storm, which resulted in both high erosion and high peak flow (Wilson, unpublished data). This suggests that the burn condition still affects rainfall runoff in the study area, although the magnitude of this effect is difficult to quantify with the limited summer rain in 2015.

6.3 Soil moisture

Similar to the issues in spatial variability with snow and rainfall data, the spatially limited and relatively small number of soil moisture sensors deployed at research catchments hampers the ability to gain a clear picture of what was occurring with soil moisture storage and subsurface flow catchment-wide. Still, data collected suggest that burned sites had greater storage of soil moisture in the uppermost 20cm of the soil profile than unburned sites.

Burned sites began WY2015 with higher antecedent moisture. This is likely due to greater rainfall totals at this site during summer 2014, though lower losses to ET, a greater storage capacity, or a combination of all three factors are also possibilities. Through the winter

months, the presence of frozen soil may be important at all sites. When soils are frozen, soil moisture declines or remains steady, suggesting that frozen soils may limit infiltration of meltwater from the snowpack. When soil thaws, soil moisture increases due to increased infiltration. Other studies have observed similar reactions during periods of frozen soil (Wilcox et al., 1997), though there is little evidence in the catchment hydrographs of IEOF from meltwater over frozen soils. UI had the shortest period of frozen soil during winter months, so meltwater infiltrated periodically during winter months to increase winter soil moisture.

High, relatively constant values for soil moisture at all sites during and immediately after snowmelt suggest that soils were at or near field capacity during this period (Figure 12). Higher soil moisture values at burned sites suggest that these sites may have greater capacity for storage in the uppermost 20cm of soil. UI shows the greatest variability in soil moisture during this period, potentially because periodic infiltration of meltwater during the winter reduced the meltwater input during spring snowmelt, led to lower and more variable spring moisture.

6.4 Runoff

6.4.1 Seasonal patterns

At all catchments, runoff was snowmelt-dominated, as snow contributed 71-86% of input. This leads to strong seasonal patterns in the hydrograph with limited flow in the winter and high flow in the spring that gradually declines through the summer. Rainfall during

summer months drives peaks in the hydrograph, though they are substantially smaller than those observed during spring snowmelt except at UI.

Because of this dominance of snowmelt input, all catchments have a strong seasonal pattern in discharge. Late spring increases in discharge reflect increased inputs to the system from snowmelt. Although this study did not directly monitor runoff mechanisms, lags between the timing of melt onset and the timing of hydrograph rise suggest that the runoff generally reaches the stream through lateral subsurface flow. Soil moisture at all sites reached field capacity between late March and mid-April, whereas the snowmelt hydrograph did not respond until the ablation of the large mid-April snow event. With this influx of meltwater, all catchments moved into spring wet, high-flux period with LSSF through hillslopes became active presumably due to deep soil moisture connectivity, as observed in McNamara et al. (2005). These high discharges were pushed to annual peaks by a period of May rainfall coming immediately following final ablation of the snowpack. From this period on, inputs to the system in the form of additional snowmelt and rainfall produced stream hydrograph response until soil moisture levels began to decline in mid-May at all catchments.

Dry periods in late May and June coincide with decreased soil moisture and discharge, with rain events causing small increases except during the period of sustained rain in July. Minor peaks in the stream hydrograph through summer months rise quickly (0.2-0.9h) and recede quickly (1.0-4.0h), suggesting small amounts of IEOF may have occurred following high intensity summer storms. For example, during the 16 August storm event the lags from peak rainfall intensity to peak discharge at UT, BT, and BI of 0.4h, 0.7h, and 0.2h, respectively, are

consistent with lags to peak caused by IEOF (Dunne, 1978). Soil moisture values support this assumption, as they remain well below field capacity throughout the rest of the summer. Only the sustained rainfall of early July appeared to reactivate LSSF and cause the summer seasonal peaks in discharge at all sites. All sites end WY2015 with very low discharge, the consequence of little rainfall through the late summer months.

6.4.2 Site comparison

UT had the highest mean and maximum elevation of all the study catchments. It experienced a persistent snowpack in winter months and had the longest snow persistence of all the study catchments. Frozen soils at this catchment may have limited the infiltration of mid-winter snowmelt, but mid-winter pulses of melt are not evident in the hydrograph. This suggests that any meltwater was stored either within the snowpack or infiltrated into the soil through thawed areas. The snowmelt runoff response was delayed at UT, but this site produced the largest total runoff. During and after snowmelt, soil moisture stayed high at UT from late March well into July, allowing for a large hydrograph response to storms in early July. UT's position as the highest elevation site and its location within the TSZ may be behind the deeper, more persistent snowpack and larger snowmelt runoff response at this catchment. It is likely that the snowpack at the highest elevations of the catchment experienced less mid-winter ablation than the monitoring site at the base of the catchment. There was only one field discharge measurement to constrain the rating curve at this site, making actual magnitudes of discharge highly uncertain, but field observations of in-stream flow and surface water ponding do support the conclusion that this site had the greatest runoff.

The lower elevation UI site experienced intermittent melt throughout winter months over mostly unfrozen soils, allowing water to continually infiltrate to the subsurface. This site also had by far the lowest runoff production of all catchments. Repetitive episodic infiltration may have increased losses to ET, limiting runoff production in this catchment. The catchment configuration is also quite different from the other study catchments, as it has a large flat valley bottom with sandy loam soil that stores moisture throughout the year (Figure 17). This soil type is unique to UI among the study catchments and was observed to be consistently wetter and less hydraulically conductive than other soils at the site or soils at other catchments. USDA classifies this soil unit as hydrologic soil group B, with 25% hydric components and a storage capacity of 16.87cm/cm, 70-86% higher than any other soil unit present at UI (USDA/NRCS, 2016). Saturated conditions were observed visually in these soils throughout summer months during WY2015. Instrumentation mounted on PVC pipe near the stream had to be adjusted regularly due to malleable saturated soil, and water was observed near the soil surface within lengths of PVC instrument mounts when instruments were adjusted. While no quantitative data were collected within this soil unit, qualitative observation leads to the suggestion that, while this sandy loam unit allows for sustained baseflow in the channel, it also acts to attenuate any snowmelt or rainfall runoff hydrograph response. Because the stream travels through a wide valley bottom, the in-stream monitoring location may also have missed some subsurface outflow from the catchment through adjacent riparian areas.

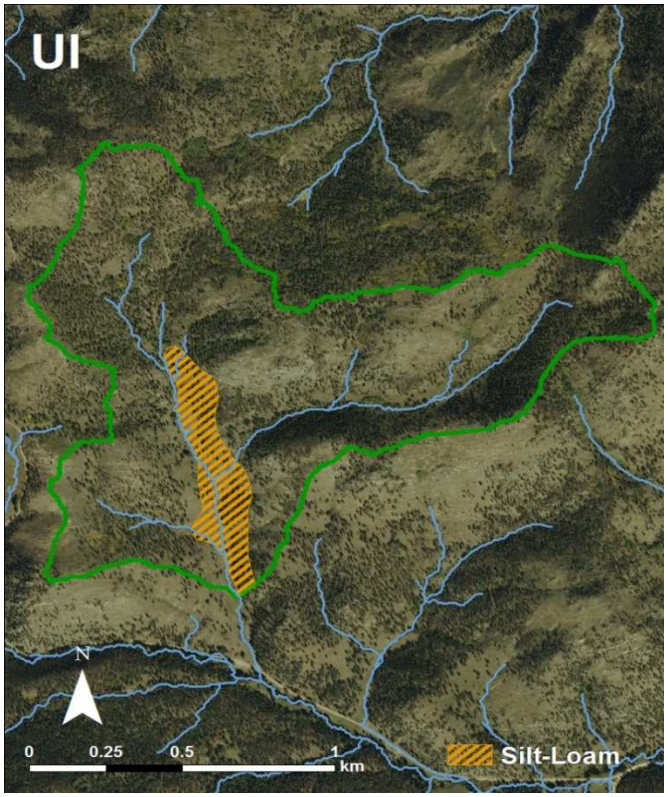

Figure 17: Map of UI highlighting silt-loam unit underlying the stream (USDA-NRCS, 2016).

The BT site had a strong snowmelt runoff hydrograph signal, similar to UT. Field observations suggest that winter flow at this catchment was limited, though problems with determining a discharge rating curve at BT resulted in a great deal of uncertainty about winter discharge at this site. BT had a rapidly rising hydrograph during spring melt, but soil moisture did not maintain levels near field capacity for nearly as long as UT, with soil moisture at BT beginning to decline below field capacity in mid-May. This may be tied to a shallower, less persistent snowpack at BT, which could have resulted from weather patterns, removal of forest canopy, lesser snow amounts tied to the lower elevation of BT, or a combination of these factors.

Regardless, this more rapid decline from field capacity in soil moisture results in an earlier recession in the hydrograph at BT and lower total runoff than observed at UT.

BI had the most responsive winter hydrograph due to intermittent melt during the winter. At the temperature monitoring location, soils were frozen during part of this time, suggesting the possibility of IEOF due to frozen soils prohibiting meltwater infiltration. The intermittent input of meltwater during the winter lessens the concentrated meltwater signal observed during spring melt at the other catchments. There is an anomalous decline in discharge at BI in mid-May that appears to have no source. The most likely explanation is equipment malfunction, as the data have been checked multiple times and the anomaly cannot be corrected using a data offset adjustment. Soil moisture begins to decline in mid-May, nearly simultaneously with soil moisture decline at BT. Discharge declines during this time as well. Discharge patterns through the summer months track very closely with those of BT, though hydrograph response to storm events shows more rapid rise to peak and decline to base flow.

Overall, UT and BI experienced the greatest amounts of discharge and similar amounts of input. These two catchments have very similar runoff ratios, despite sharing neither the same burn status nor the same snow zone. However, the timing of inputs and discharge at these sites is very different. UT experiences most of its input during winter months and most of its discharge beginning with spring snowmelt. This pattern of input and discharge timing is echoed at the other TSZ site, BT, though the magnitude of the runoff ratio is 22% smaller due to shallower, less persistent snowpack. BI also gets most of its input during winter months, but the pattern of discharge is not seasonally confined, with discharge responding to input

throughout the year. A shallower, denser snowpack experiencing periodic ablation at an ISZ site resulted in a similar runoff ration to a TSZ site with a deeper, more persistent snowpack that ablated at the end of spring. UI is the oddity again, likely because of the increased storage in the valley bottom silt loam that led to the very small runoff ratio.

The complex interactions of snow accumulation and ablation with freezing soil and runoff generation make it difficult to draw any solid conclusions in the comparison of runoff from burned and unburned catchments. The burned catchments were also monitored 3 years after burning, which may have limited differences between burned and unburned catchments. Moody and Martin (2001) and Pierson et al. (2001) both suggest that 3-5yrs of recovery return burned plots to pre-fire infiltration conditions. Peak discharge differences after burning may have a wider window of time, with studies suggesting 2-7yrs for return to pre-fire conditions (Brown, 1972), but the water year studied did not include a large enough rain event to cause a high hydrograph peak. Changes in ET during the recovery are uncertain, with some studies suggesting that post-fire ET may be very similar to pre-fire ET (Flerchinger & Seyfried, 2012). However, other research suggests that changes in vegetation induced by fire may continue to have an effect as long as ten years after the fire (Montes-Helu et al., 2009). Higher soil moisture at the onset of WY2015 in the burned sites supports the possibility of lower ET at these sites, but these differences may also be due to varying antecedent precipitation and moisture storage capacity at the monitoring sites.

7 CONCLUSIONS

This research examined how the timing and magnitude of rainfall and snowmelt runoff in catchments at the intermittent-persistent transition were affected by wildfire. At four study catchments that encompassed burned and unburned status and transitional and intermittent snow zone conditions, runoff was dominated by snowmelt moving via LSSF to the stream channel. Intermittent pulses of meltwater were introduced to the system at burned and lower elevation catchments by periodic snow ablation during winter months. However, most melt water entered the the catchment hydrologic regimes during a final spring snowmelt event in April as catchments transitioned from snow-dominated winter/spring conditions to rain-dominated summer conditions. Infiltration of meltwater pushed soil moisture above field capacity, resulting in connectivity in soil moisture reservoirs and the activation of LSSF through steep hillslopes. Rainfall also contributed to runoff to a lesser degree in the forms of high intensity summer storms that produced IEOF.

Snow accumulation and ablation showed similar patterns at all sites, though the highest elevation unburned site had greater snow persistence than the other three sites. Burned sites and the relatively open canopy UI had greater mid-winter ablation than UT, possibly due to the absence of canopy cover and greater solar insolation. Snow density was higher at burned sites than at unburned sites, suggesting that the removal of canopy may also contribute to an increase in snow density. Rainfall totals were higher at unburned sites due to differences in prevailing weather patterns for the summer of WY2015. High intensity rainfall produced the majority of summer runoff at each catchment, though high intensity events were much more

common at unburned catchments than burned catchments. Overall input from snowmelt and rainfall was very similar at all catchments, with snowmelt contributing 71-86% of the input.

Soil moisture storage patterns in the uppermost 20cm of soil were also similar at all catchments, with a period of low soil moisture during winter followed by soil moisture at or near field capacity during spring melt and a steady decline through drier summer months. However, burned sites had overall higher soil moisture throughout the year, including during mid-winter months. This difference may relate to burning effects, but this is not certain due to the small number of soil moisture monitoring sites in each catchment. Discharge patterns at all sites were dominated by spring snowmelt peaks, though the magnitude of these peaks varied by site. TSZ catchments both had low discharge during winter months with a marked increase and peak during spring melt. ISZ catchments were both more variable throughout the year because mid-winter melt also contributed to discharge. Although the number of catchmcents sampled is small, results show that high runoff ratios in this region can develop from either more persistent snow (UT) or more intermittent melt water input throughout the winter (BI).

In addition, frozen soils appear to have some effect as well on snowmelt runoff, as the longer period of frozen soils at UT coincides with a later, larger magnitude input of snowmelt during the spring. Regardless of the effect of canopy cover and frozen soil, it is apparent that the longer soil moisture stays at or near field capacity, the longer the duration and greater the magnitude of spring snowmelt discharge response.

While it is sometimes necessary and often expedient to universalize the effects of wildfire on the hydrologic regime of a catchment, this research suggests that regional and site

specific characteristics can result in unexpected outcomes. The hydrologic regime of each catchment showed individualized reaction to inputs, suggesting that a holistic view of the variables driving hydrologic processes at these catchments is warranted. The cumulative effects of wildfire, post-wildfire recovery, and elevation-driven snow persistence resulted in differences in the hydrologic regimes of each catchment that rendered clean comparison of runoff responses difficult. However, the beginning of a better understanding of differences in and changes to the hydrology of these catchments in the Colorado Front Range gives context to prior research.

Further research monitoring post-fire hydrologic change should begin immediately after a burn and include more study catchments that are monitored over multiple years. All variables should be monitored at more locations in each catchment to capture intra-catchment variability in insolation, slope, and aspect. If feasible, site characteristics should be more closely matched, including elevation, slope, aspect, and vegetation cover, with pre-fire vegetation at burned sites matching that of unburned sites. Both greater measurement density and better pairing of catchment storm patterns and characteristics would help clarify the roles of both fire-effect status and snow zones in differences between research catchments.

REFERENCES

ARS (Agriculture Research Service). 2015. Rainfall Intensity Summarization Tool (RIST) (Version 3.94) [computer software]. United States Department of Agriculture. Retrieved from http://www.ars.usda.gov/Research/docs.htm?docid=3254

BAER (Burned Area Emergency Response). 2012. High Park Fire Burned Area Emergency Response (BAER) Report. High Park Fire Emergency Stabilization Plan, 12 July 2012

Arcement GJ, Schneider VR. 1989. Guide for selecting Manning's roughness coefficients for natural channels and flood plains. *U.S. Geological Survey Water-Supply Paper* **2339**

Bayard D, Stähli M, Parriaux A, Flühler H. 2005. The influence of seasonally frozen soil on the snowmelt runoff at two Alpine sites in southern Switzerland. *Journal of Hydrology* **309** (1-4): 66–84 DOI: 10.1016/j.jhydrol.2004.11.012

Benson MA, Dalrymple T. 1967. General field and office procedures for indirect measurements. *U.S. Geological Survey Techniques of Water-Resources Investigations,* book 3, chap. A1, 30 p., http://pubs.er.usgs.gov/publication/twri03A1

Benavides-Solorio JDD, MacDonald LH. 2005. Measurement and prediction of post-fire erosion at the hillslope scale, Colorado Front Range. *International Journal of Wildland Fire* **14** (4): 457 DOI: 10.1071/WF05042

Blumberg, EJ. 2012. Spatial Variability of Snow Depth Measurements at Two Mountain Pass Snow Telemetry Stations. Unpublished M.S. thesis, Geosciences, Colorado State University, Fort Collins, Colorado, USA.

Brown JAH. 1972. Hydrologic effects of a brushfire in a catchment in south-eastern New South Wales. *Journal of Hydrology* **15**: 77-96 DOI: 10.1016/0022-1694(72)90077-7

Burles K, Boon S. 2011. Snowmelt energy balance in a burned forest plot, Crowsnest Pass, Alberta, Canada. *Hydrological Processes* **25**: 3012–3029 DOI: 10.1002/hyp.8067

Colorado Climate Center. 2015. Customizable data plots. Colorado State University. Retrieved from http://climate.colostate.edu/~autowx/fclwx_plotsearch_form.php

Drake E, DeSisto C, McDonald S, Evans S, Barry D, Baccus, B. 2008. Untangling Climate and Wildfire Influences from Snow Water Equivalent Measurements on the Deer Park, WA Snow Course, in: Proceedings of the Western Snow Conference, 15-17 April, Hood River, Oregon, 2008.

Dunkerley D. 2012. Effects of rainfall intensity fluctuations on infiltration and runoff: rainfall simulation on dryland soils, Fowlers Gap, Australia. *Hydrological Processes* 26 (15): 2211-2224 DOI: 10.1002/hyp.8317

Dunne T. 1978. Field studies of hillslope flow processes. *Hillslope Hydrology* 227: 227-293

Dunne T, Black RD. 1970. An Experimental Investigation of Runoff Production in Permeable Soils. *Water Resources Research* **6** (2): 478-490 DOI: 10.1029/WR006i002p00478

Dunne T, Black RD. 1971. Runoff processes during snowmelt. *Water Resources Research* **7** (5): 1160-1172

Ebel BA, Hinckley ES, Martin DA. 2012. Soil-water dynamics and unsaturated storage during snowmelt following wildfire. *Hydrology and Earth System Sciences* **16** (5): 1401–1417 DOI: 10.5194/hess-16-1401-2012

Fassnacht SR. 2004. Estimating Alter-shielded gauge snowfall undercatch, snowpack sublimation, and blowing snow transport at six sites in the coterminous USA. *Hydrological Processes* 18: 3481-3492 DOI: 10.1002/hyp.5806

Flerchinger GN, Seyfried MS. 2012. Measurement and Modeling of Evapotranspiration Before and After Prescribed Fire and Vegetation Removal. *AGU Fall Meeting Abstracts, Vol. 1*

García-Corona R, Benito E, de Blas E, Varela ME. 2004. Effects of heating on some soil physical properties related to its hydrological behaviour in two north-western Spanish soils. *International Journal of Wildland Fire* **13** (2): 195–199 DOI: 10.1071/WF03068

Harpold AA, Biederman JA, Condon K, Merino M, Korgaonkar Y, Nan T, Sloat LL, Ross M, Brooks PD. 2014. Changes in snow accumulation and ablation following the Las Conchas Forest Fire, New Mexico, USA. *Ecohydrology* **7** (2): 440–452 DOI: 10.1002/eco.1363

Hedstrom NR, Pomeroy JW. 1998. Measurements and modelling of snow interception in the boreal forest. *Hydrological Processes* **12** (10/11): 1611-1625 DOI: 10.1002/(SICI)1099-1085(199808/09)12:10/11<1611::AID-HYP684>3.0.CO;2-4

Hinckley E-LS, Ebel BA, Barnes RT, Anderson RS, Williams, MW, Anderson, SP. 2014. Aspect control of water movement on hillslopes near the rain-snow transition of the Colorado Front Range. *Hydrological Processes* **28** (1): 74-85 DOI: 10.1002/hyp.9549

Hunsaker CT, Whitaker TW, Bales RC. 2012. Snowmelt Runoff and Water Yield Along Elevation and Temperature Gradients in California's Southern Sierra Nevada1. *JAWRA Journal of the American Water Resources Association* **48** (4): 667–678 DOI: 10.1111/j.1752-1688.2012.00641.x

Kampf S, Markus J, Heath J, Moore C. 2015. Snowmelt runoff and soil moisture dynamics on steep subalpine hillslopes. *Hydrological Processes* **29** (5): 712–723 DOI: 10.1002/hyp.10179

Kashipazha AH. 2012. *Practical snow depth sampling around six snow telemetry (SNOTEL) stations in Colorado and Wyoming, United States.* Unpublished M.S. thesis, Watershed Science, Colorado State University, Fort Collins, Colorado, USA.

Kilpatrick FA, Cobb ED. 1985. Measurement of discharge using tracers. *U.S. Geological Survey Techniques of Water-Resources Investigations,* book 3, chap. A16, 52 p. http://pubs.usgs.gov/twri/twri3-a16/

Linderson M-L. 2003. Spatial Distribution of Meso-Scale Precipitation in Scania, Southern Sweden. *Geografiska Annaler: Series A, Physical Geography* **85**: 183-196 DOI: 10.1111/1468-0459.00197

Lopes VL, Ffolliott PF. 1993. Sediment Rating Curves for a Clearcut Ponderosa Pine Watershed in Northern Arizona. *Journal of the American Water Resources Association* **29** (3): 370-382 DOI: 10.1111/j.1752-1688.1993.tb03214.x

Manning, R. 1889. On the flow of water in open channels and pipes. *Institution of Civil Engineers, Ireland* **20**: 161-207

Martin DA, Moody JA. 2001. Comparison of soil infiltration rates in burned and unburned mountainous watersheds. *Hydrological Processes* **15** (15): 2893–2903 DOI: 10.1002/hyp.380

Martinez-Meza E, Whitford WG. 1996. Stemflow, throughfall and channelization of stemflow by roots in three Chihuahuan desert shrubs. *Journal of Arid Environments* **32** (3): 271-287 DOI: 10.1006/jare.1996.0023

McNamara JP, Chandler D, Seyfried M, Achet S. 2005. Soil moisture states, lateral flow, and streamflow generation in a semi-arid, snowmelt-driven catchment. *Hydrological Processes* **19** (20): 4023–4038 DOI: 10.1002/hyp.5869

Molotch NP, Brooks PD, Burns SP, Litvak M, Monson RK, McConnell JR, Musselman K. 2009. Ecohydrological controls on snowmelt partitioning in mixed-conifer sub-alpine forests. *Ecohydrology* **2** (2): 129-142 DOI: 10.1002/eco.48

Montes-Helu MC, Kolb T, Dore S, Sullivan B, Hart SC, Koch G, Hungate BA. 2009. Persistent effects of fire-induced vegetation change on energy partitioning and evapotranspiration in ponderosa pine forests. *Agricultural and Forest Meteorology* **149** (3-4): 491-500 DOI10.1016/j.agrformet.2008.09.011

Moody JA, Ebel BA. 2014. Infiltration and runoff generation processes in fire-affected soils. *Hydrological Processes* **28** (9): 3432-3453 DOI: 10.1002/hyp.9857

Moody JA, Dungan Smith J, Ragan BW. 2005. Critical shear stress for erosion of cohesive soils subjected to temperatures typical of wildfires. *Journal of Geophysical Research: Earth Surface* **110**: 1–13 DOI: 10.1029/2004JF000141

Moody JA, Martin DA. 2001. Initial Hydrologic and Geomorphic Response Following a Wildfire in the Colorado Front Range. **1070**: 1049–1070

Moore C, Kampf S, Stone B, Richer E. 2015. A GIS-based method for defining snow zones: application to the western United States. *Geocarto International* **30** (1): 62-81 DOI: 10.1080/10106049.2014.885089

Osborn HB, Lane LJ, Hundley JF. 1972. Optimum gaging of thunderstorm rainfall in southeastern Arizona. *Water Resources Research* **8** (1): 259–265 DOI: 10.1029/WR008i001p00259

Pierson FB, Robichaud PR, Spaeth KE. 2001. Spatial and temporal effects of wildfire on the hydrology of a steep rangeland watershed. *Hydrological Processes* **15** (15): 2905–2916 DOI: 10.1002/hyp.381

PRISM Climate Group. 2015. Oregon State University. Retrieved from http://prism.oregonstate.edu, created 4 Feb 2004

Richer E, Kampf S. 2013. Estimating source regions for snowmelt runoff in a Rocky Mountain basin: tests of a data-based conceptual modeling approach. *Hydrological Processes* **28** (4): 2237-2250 DOI: 10.1002/hyp.9751

Robichaud PR. 2000. Fire effects on infiltration rates after prescribed fire in Northern Rocky Mountain forests, USA. *Journal of Hydrology* **231-232**: 220–229 DOI: 10.1016/S0022-1694(00)00196-7

Robichaud PR. 2005. Measurement of post-fire hillslope erosion to evaluate and model rehabilitation treatment effectiveness and recovery. *International Journal of Wildland Fire* **14** (4): 475 DOI: 10.1071/WF05031

Schmeer S. 2014. Post-fire erosion response and recovery, High Park Fire, Colorado. Master's thesis, Colorado State University, Fort Collins, CO Retrieved from https://dspace.library.colostate.edu/handle/10217/84140

Seyfried MS, Grant LE, Marks D, Winstral A, McNamara J. 2009. Simulated soil water storage effects on streamflow generation in a mountainous snowmelt environment, Idaho, USA. *Hydrological Processes* **23**: 858-873 DOI: 10.1002/hyp.7211

Shakesby R, Doerr S. 2006. Wildfire as a hydrological and geomorphological agent. *Earth-Science Reviews* **74** (3-4): 269–307 DOI: 10.1016/j.earscirev.2005.10.006

Smith RS, Moore RD, Weiler M, Jost G. 2014. Spatial controls on groundwater response dynamics in a snowmelt-dominated montane catchment. *Hydrology and Earth System Sciences* **18** (5): 1835–1856 DOI: 10.5194/hess-18-1835-2014

Stone B. 2015. Mapping burn severity, pine beetle infestation, and their interatction at the High Park Fire. Unpublished M.S. thesis, Ecology, Colorado State University, Fort Collins, CO Retrieved from https://dspace.library.colostate.edu/handle/10217/167258

USDA-NRCS (U.S. Department of Agriculture - Natural Resources Conservation Service). 2013. Web Soil Survey. Retrieved from http://websoilsurvey.sc.egov.usda.gov/App/WebSoilSurvey.apx

Wagenbrenner JW, MacDonald LH, Rough D. 2006. Effectiveness of three post-fire rehabilitation treatments in the Colorado Front Range. *Hydrological Processes* **20** (14): 2989–3006 DOI: 10.1002/hyp.6146

Westerling AL, Hidalgo HG, Cayan DR, Swetnam TW. 2006. Warming and earlier spring increase western U.S. forest wildfire activity. *Science* **313** (5789): 940–3 DOI: 10.1126/science.1128834

Wilcox BP, Newman BD, Brandes D, Davenport DW, Reid K. 1997. Runoff from a semiarid Ponderosa pine hillslope in New Mexico. *Water Resources Research* **33** (10): 2301 DOI: 10.1029/97WR01691

Williams CJ, McNamara JP, Chandler DG. 2009. Controls on the temporal and spatial variability of soil moisture in a mountainous landscape: the signature of snow and complex terrain. *Hydrology and Earth System Sciences* **13** (7): 1325–1336 DOI: 10.5194/hess-13-1325-2009

Winkler RD. 2011. Changes in Snow Accumulation and Ablation after a Fire in South- central British Columbia. *Streamline Watershed Management Bulletin* **14** (2)

APPENDICES

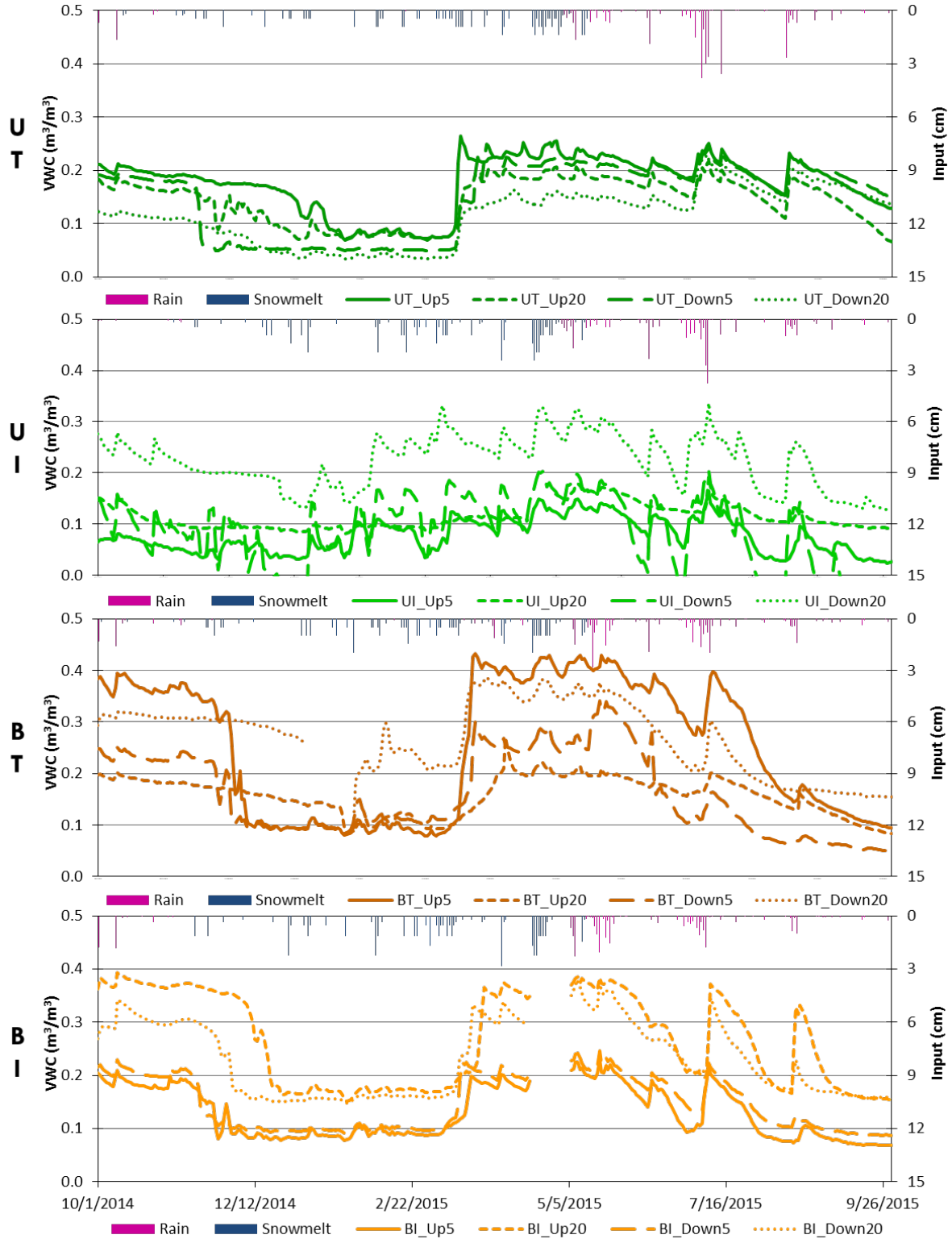

Figure 18: Time series of soil moisture from each of four individual soil moisture sensors at each catchment and input for WY2015.

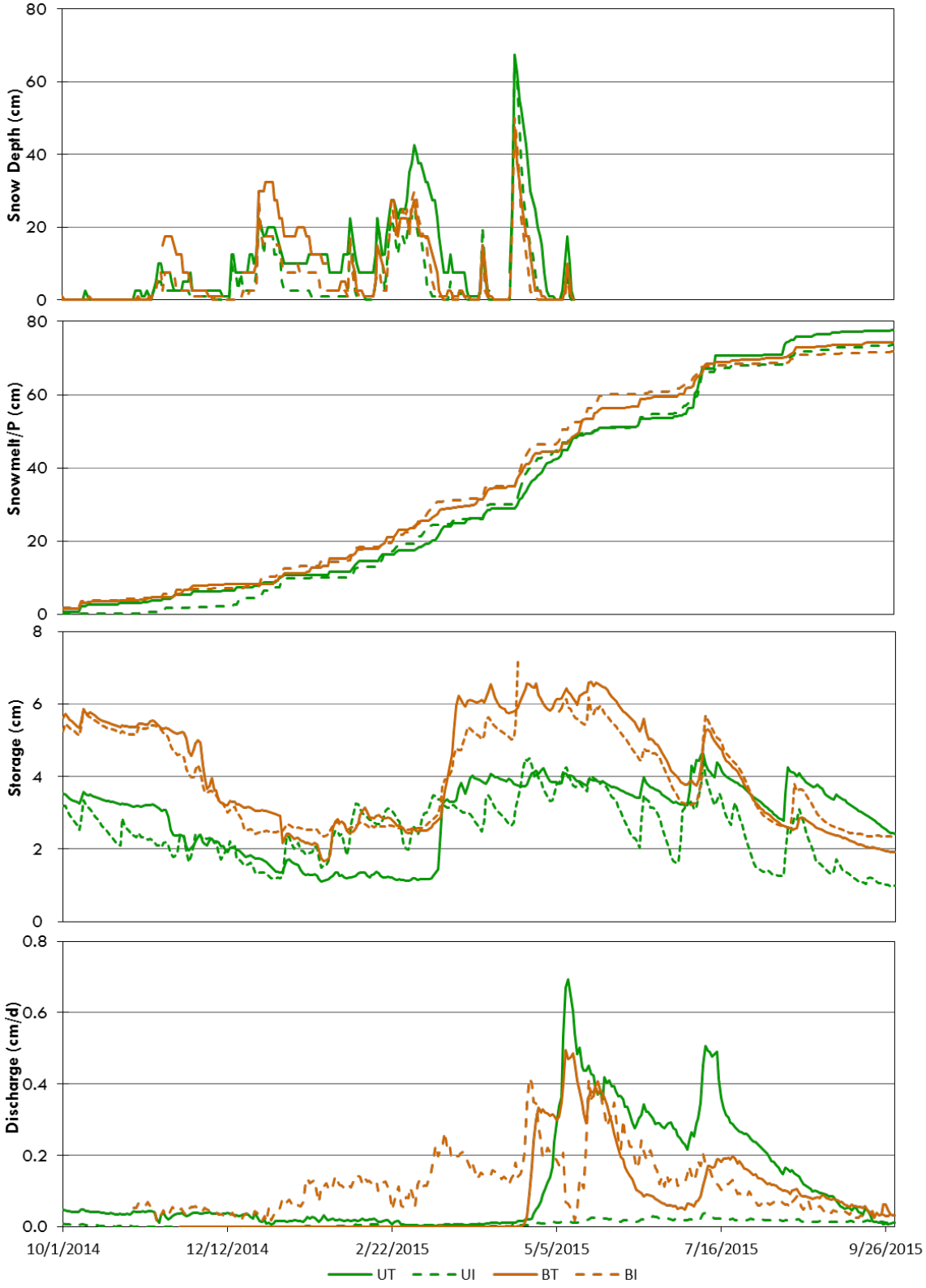

Figure 19: Snow depth, cumulative input, storage, and normalized discharge time series for each catchment.

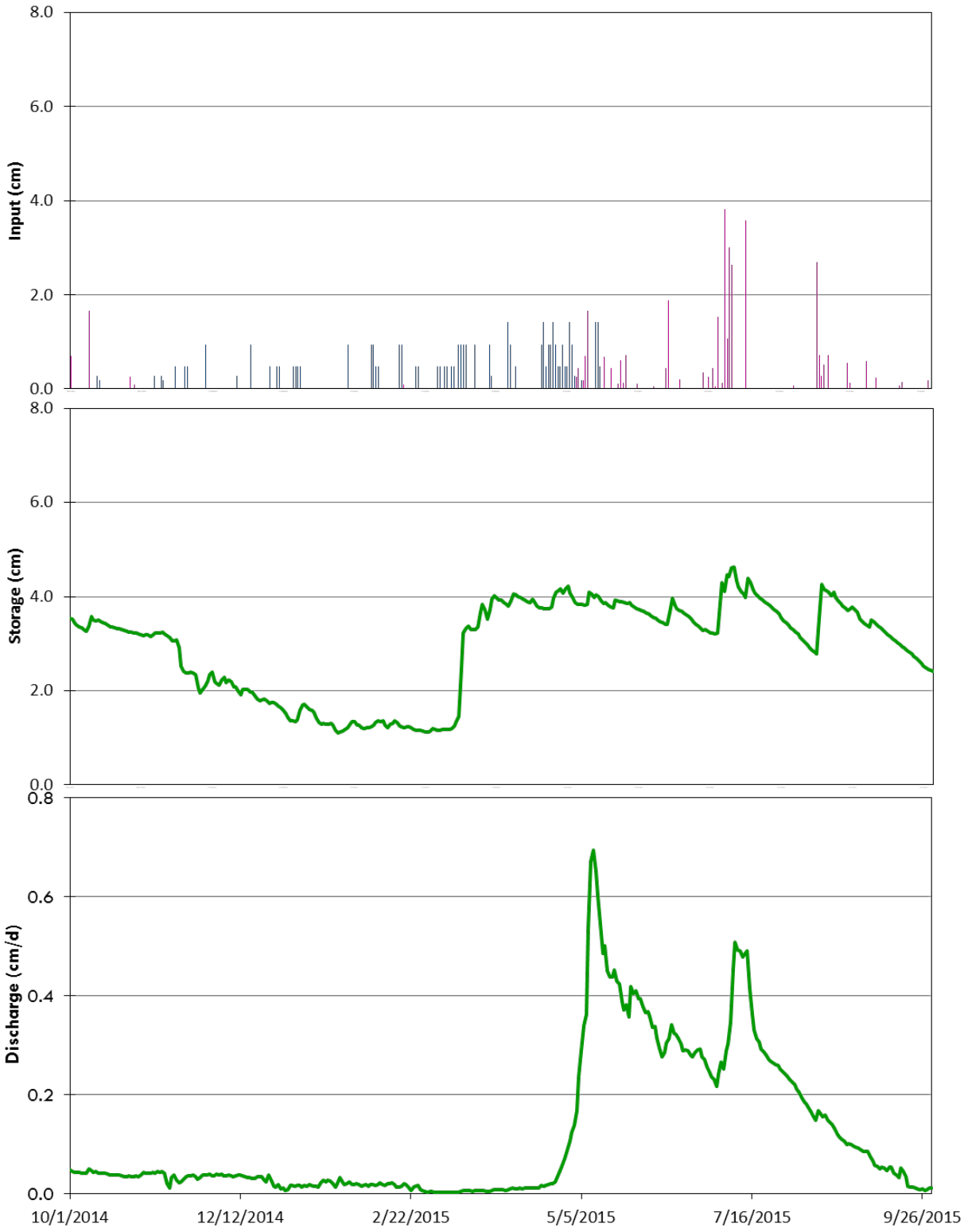

Figure 20: Input as snowmelt (blue) and rainfall (purple), soil moisture storage, and normalized discharge for WY2015 at UT.

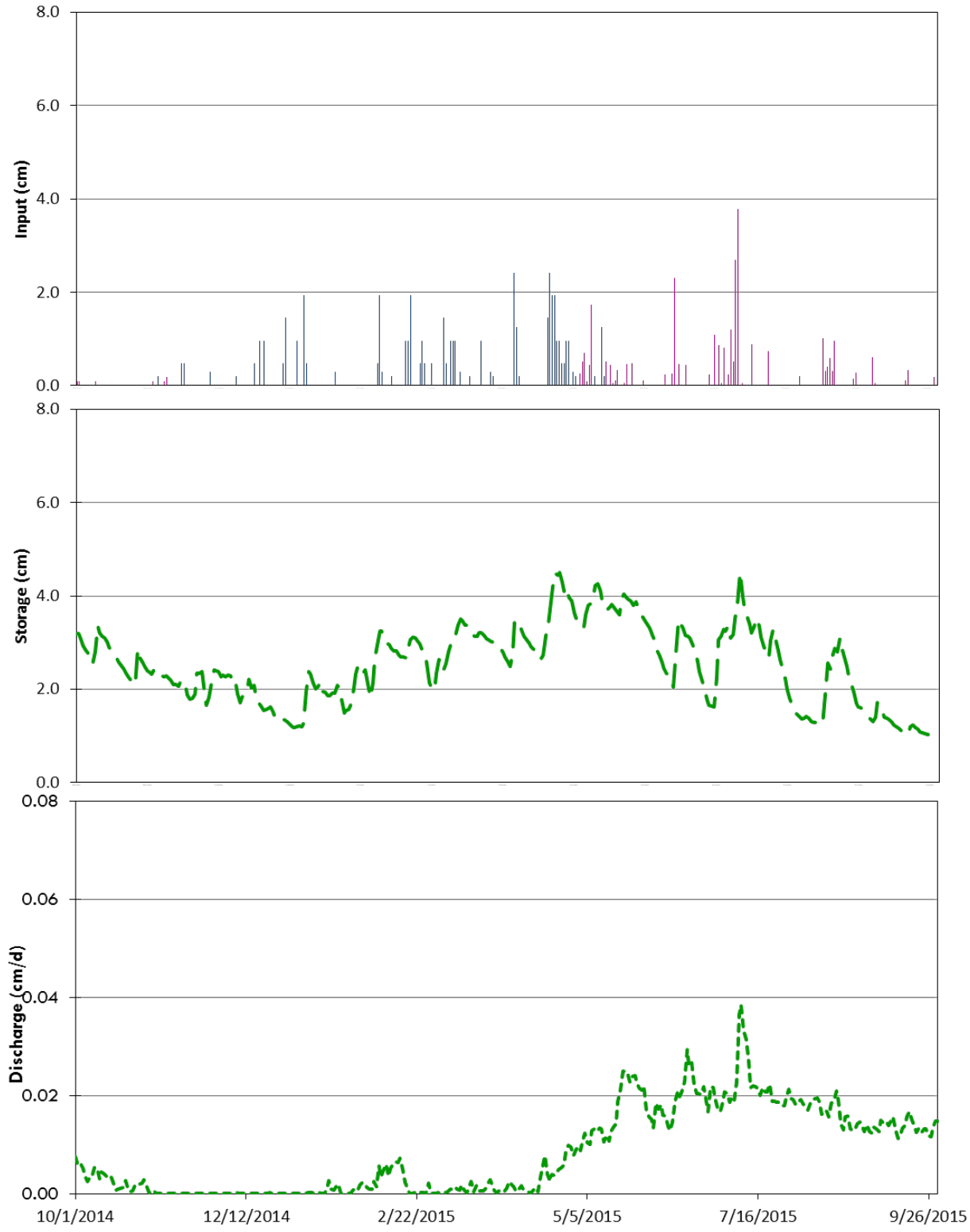

Figure 21: Input as snowmelt (blue) and rainfall (purple), soil moisture storage, and normalized discharge for WY2015 at UI; note that the scale for discharge has been decreased by one order of magnitude to show detail.

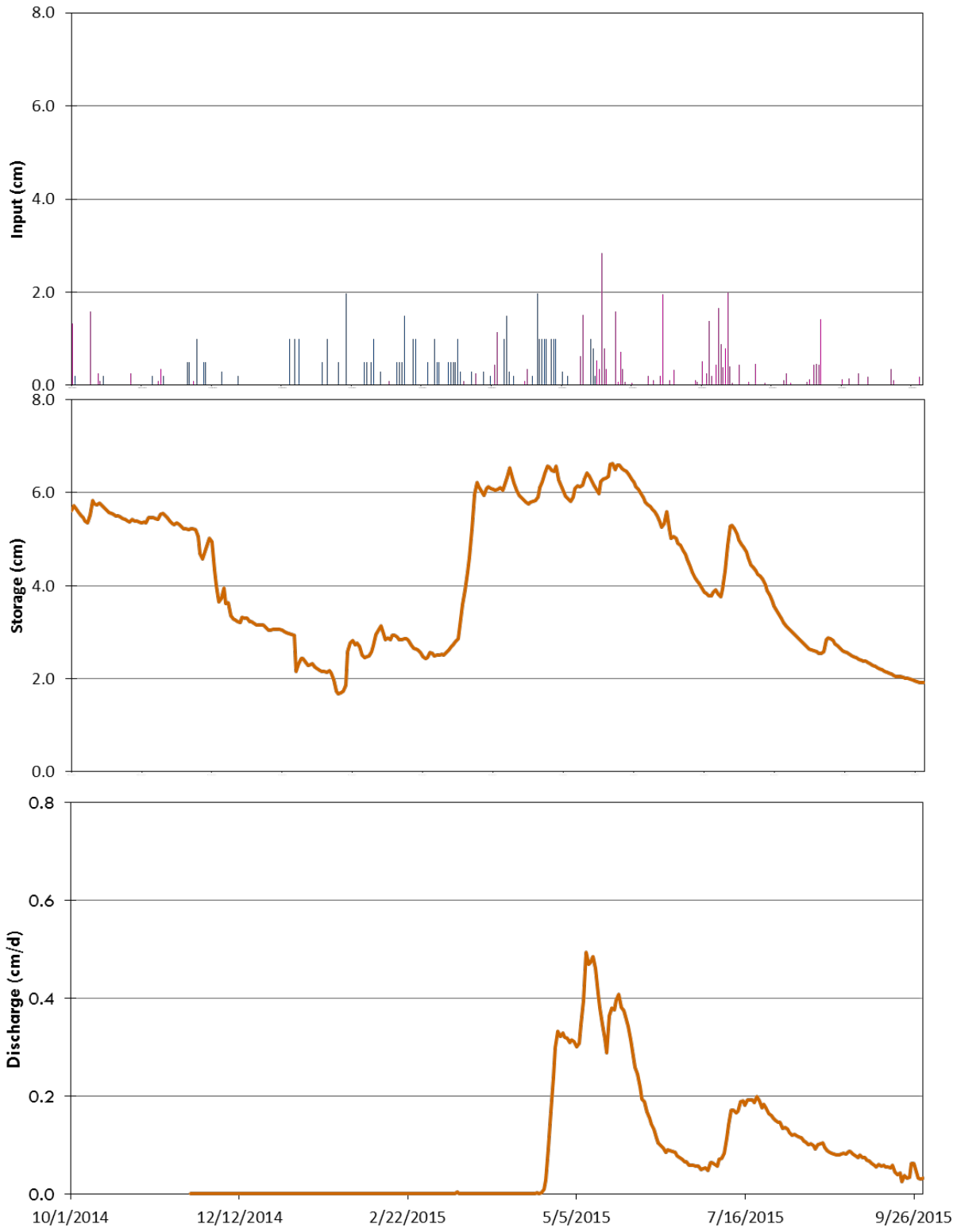

Figure 22: Input as snowmelt (blue) and rainfall (purple), soil moisture storage, and normalized discharge for WY2015 at BT.

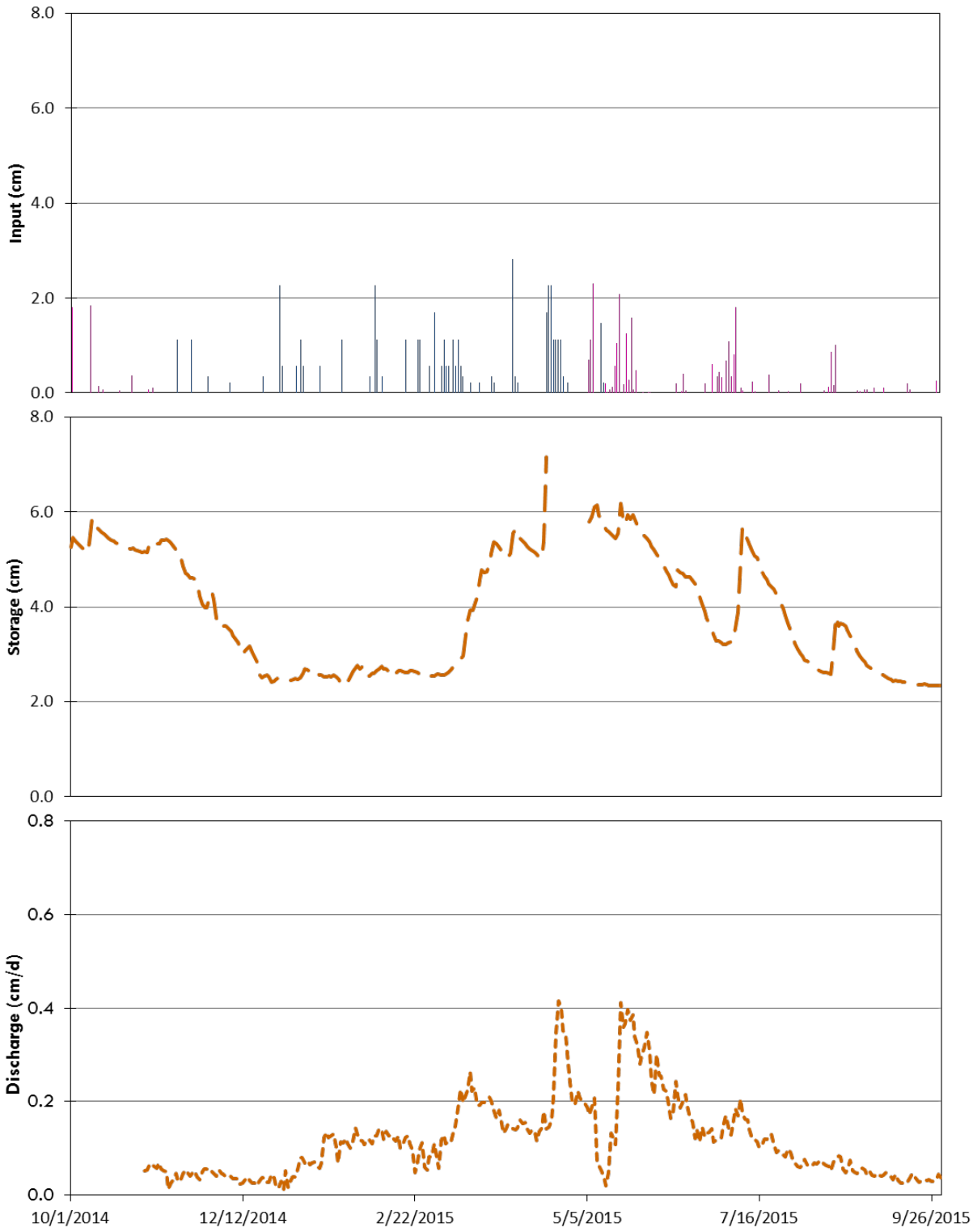

Figure 23: Input as snowmelt (blue) and rainfall (purple), soil moisture storage, and normalized discharge for WY2015 at BT.

Table 11: Summary statistics for all storms with I_{30}>1.0cm/h at UT

UT						
Gauge	Date	Total P (cm)	Duration (h)	Max I_5 (cm/h)	Max I_{30} (cm/h)	Lag, peak P to peak Q (h)
UT_TB1	6/11/2015	1.8	11.4	1.5	1.1	3.33
UT_TB1	7/2/2015	1.5	7.0	10.7	2.4	0.17
UT_TB1	7/5/2015	3.8	7.0	5.2	2.4	2.33
UT_TB1	7/7/2015	2.9	8.8	5.8	2.7	0.33
UT_TB1	7/14/2015	3.6	7.2	10.1	3.7	0.25
UT_TB1	8/13/2015	2.7	4.4	10.1	4.9	0.33
UT_TB1	8/14/2015	0.7	0.2	6.7	1.4	0.42
UT_TB1	8/16/2015	0.5	0.3	4.9	1.0	0.42
UT_TB2	8/13/2015	1.9	4.3	8.3	3.4	0.25
UT_TB2	8/16/2015	1.2	4.0	11.3	2.4	0.33
UT_TB2	8/26/2015	1.1	1.7	2.7	1.6	0.25
Averages		**2.0**	**5.1**	**7.0**	**2.5**	**0.76**

Table 12: Summary statistics for all storms with I_{30}>1.0cm/h at UI

UI						
Gauge	Date	Total P (cm)	Duration (h)	Max I_5 (cm/h)	Max I_{30} (cm/h)	Lag, peak P to peak Q (h)
UI_TB1	6/11/2015	2.1	11.8	2.7	1.1	2.00
UI_TB1	6/30/2015	0.9	6.3	2.7	1.4	0.50
UI_TB1	7/2/2015	0.8	2.7	5.5	1.5	0.08
UI_TB1	7/7/2015	2.6	8.4	4.3	2.4	0.67
UI_TB1	7/8/2015	3.8	18.6	4.3	1.6	0.58
UI_TB1	7/14/2015	0.9	7.2	2.4	1.1	0.50
UI_TB1	7/21/2015	0.7	1.5	5.5	1.3	0.42
UI_TB1	8/13/2015	1.0	3.5	4.0	1.9	0.42
UI_TB1	8/16/2015	0.6	0.3	4.3	1.1	0.92
UI_TB2	7/5/2015	1.2	10.6	3.8	1.0	4.92
UI_TB2	7/7/2015	5.0	28.5	3.6	1.3	2.75
UI_TB2	7/21/2015	0.7	1.4	6.5	1.4	0.42
UI_TB2	8/13/2015	1.1	4.2	4.6	2.1	0.42
UI_TB2	8/16/2015	0.8	0.2	8.6	1.6	0.92
Averages		**1.6**	**7.5**	**4.5**	**1.5**	**1.11**

Table 13: Summary statistics for all storms with I_{30}>1.0cm/h at BT

BT						
Gauge	Date	Total P (cm)	Duration (h)	Max I_5 (cm/h)	Max I_{30} (cm/h)	Lag, peak P to peak Q (h)
BT_TB1	7/1/2015	1.4	1.0	8.5	2.6	0.42
BT_TB2	8/16/2015	0.5	0.5	2.8	1.0	0.67
Averages		**1.0**	**0.7**	**5.7**	**1.8**	**0.55**

Table 14: Summary statistics for all storms with an I_{30}>1.0cm/h at BI

BI						
Gauge	Date	Total P (cm)	Duration (h)	Max I_5 (cm/h)	Max I_{30} (cm/h)	Lag, peak P to peak Q (h)
BI_TB1	6/28/2015	0.6	0.4	3.7	1.2	0.17
BI_TB1	8/16/2015	0.9	0.6	5.8	1.7	0.17
BI_TB2	7/1/2015	0.6	0.9	3.4	1.1	0.25
Averages		**0.7**	**0.6**	**4.3**	**1.3**	**0.20**